Article

Neuron

Targeted Ablation, Silencing, and Activation Establish Glycinergic Dorsal Horn Neurons as Key Components of a Spinal Gate for Pain and Itch

Highlights

- Glycinergic dorsal horn neurons exert segmental control over pain and itch
- Their local inhibition causes hyperalgesia and signs of spontaneous discomfort
- Local activation reduces acute pain, neuropathic hyperalgesia, and chemical itch

Authors

Edmund Foster, Hendrik Wildner, ..., Michael Bösl, Hanns Ulrich Zeilhofer

Correspondence

zeilhofer@pharma.uzh.ch

In Brief

Foster et al. establish dorsal horn glycinergic neurons as critical elements of a spinal gate for pain and itch. Silencing and ablation of these neurons induces local hyperalgesia and spontaneous discomfort, whereas their activation alleviates pain and itch.

Foster et al., 2015, Neuron *85*, 1289–1304
March 18, 2015
http://dx.doi.org/10.1016/j.neuron.2015.02.028

CellPress

Neuron
Article

Targeted Ablation, Silencing, and Activation Establish Glycinergic Dorsal Horn Neurons as Key Components of a Spinal Gate for Pain and Itch

Edmund Foster,[1,5] Hendrik Wildner,[1,5] Laetitia Tudeau,[1,4] Sabine Haueter,[1,4] William T. Ralvenius,[1] Monika Jegen,[1,4] Helge Johannssen,[1] Ladina Hösli,[1] Karen Haenraets,[1,4] Alexander Ghanem,[2] Karl-Klaus Conzelmann,[2] Michael Bösl,[3] and Hanns Ulrich Zeilhofer[1,4,*]

[1]Institute of Pharmacology and Toxicology, University of Zurich, Winterthurerstrasse 190, 8057 Zürich, Switzerland
[2]Gene Center, Ludwig Maximilians University Munich, Max von Pettenkofer Institute of Virology, Feodor Lynen Strasse 25, 81377 Munich, Germany
[3]Experimental Biomedicine, University of Würzburg, Josef Schneider Strasse 2, 97080 Würzburg, Germany
[4]Institute of Pharmaceutical Sciences, Swiss Federal Institute of Technology (ETH) Zürich, Vladimir Prelog Weg 4, 8093 Zürich, Switzerland
[5]Co-first author
*Correspondence: zeilhofer@pharma.uzh.ch
http://dx.doi.org/10.1016/j.neuron.2015.02.028

SUMMARY

The gate control theory of pain proposes that inhibitory neurons of the spinal dorsal horn exert critical control over the relay of nociceptive signals to higher brain areas. Here we investigated how the glycinergic subpopulation of these neurons contributes to modality-specific pain and itch processing. We generated a GlyT2::Cre transgenic mouse line suitable for virus-mediated retrograde tracing studies and for spatially precise ablation, silencing, and activation of glycinergic neurons. We found that these neurons receive sensory input mainly from myelinated primary sensory neurons and that their local toxin-mediated ablation or silencing induces localized mechanical, heat, and cold hyperalgesia; spontaneous flinching behavior; and excessive licking and biting directed toward the corresponding skin territory. Conversely, local pharmacogenetic activation of the same neurons alleviated neuropathic hyperalgesia and chloroquine- and histamine-induced itch. These results establish glycinergic neurons of the spinal dorsal horn as key elements of an inhibitory pain and itch control circuit.

INTRODUCTION

Pain evoked in response to potentially tissue-damaging stimuli is essential for the maintenance of our physical integrity. It can, however, have a severe impact on our well-being when it occurs spontaneously or in response to inappropriate stimuli. It is widely accepted that the spinal dorsal horn, which constitutes the first site for synaptic processing in the pain pathway, serves a critical role for maintaining a physiological level of pain sensitivity. Conversely, maladaptive changes at this site contribute critically to a wide variety of pain pathologies (Kuner, 2010; Sandkühler, 2009; Woolf and Salter, 2000; Zeilhofer et al., 2012). The concept of the dorsal horn as a first site to control the modality and intensity of sensory signals conveyed to higher CNS centers dates back to Wall and Melzack's gate control theory of pain (Melzack and Wall, 1965). According to their theory, inhibitory dorsal horn interneurons would constitute the physical basis of this pain gate. They would become activated primarily by input from (non-nociceptive) low-threshold myelinated sensory nerve fibers and would, in turn, control the activity of spinal output neurons.

Early work with antagonists of inhibitory neurotransmitter receptors has demonstrated that exaggerated pain responses can be triggered by blocking inhibitory neurotransmission in the spinal cord (Beyer et al., 1985; Loomis et al., 2001; Sherman and Loomis, 1994; Sivilotti and Woolf, 1994; Yaksh, 1989). More recent work has suggested that diminished inhibitory control over dorsal horn sensory circuits leads to increased excitability and spontaneous activity of dorsal horn neurons (Drew et al., 2004; Sorkin et al., 1998) and allows the excitation of normally pain-specific neurons by inappropriate (non-nociceptive) signals (Baba et al., 2003; Keller et al., 2007; Torsney and MacDermott, 2006; for a review see Sandkühler, 2009). A large body of evidence, meanwhile, indicates that diminished synaptic inhibition also occurs naturally in the course of inflammatory and neuropathic syndromes through various mechanisms (Zeilhofer et al., 2012).

Inhibitory interneurons make up about one-third of the total neuronal population in the spinal dorsal horn. These neurons use either γ-aminobutyric acid (GABA) or glycine or both for fast neuronal inhibition. In the superficial dorsal horn, i.e., in the termination area of nociceptors, the majority of inhibitory neurons are purely GABAergic, whereas those in the deep dorsal horn are mainly mixed GABA/glycinergic neurons (Todd and Spike, 1993; for a review, see Zeilhofer et al., 2012). Despite recent progress (Duan et al., 2014), the circuits and interneuron types contributing to spinal pain control are still not completely understood. A detailed and comprehensive analysis has so far

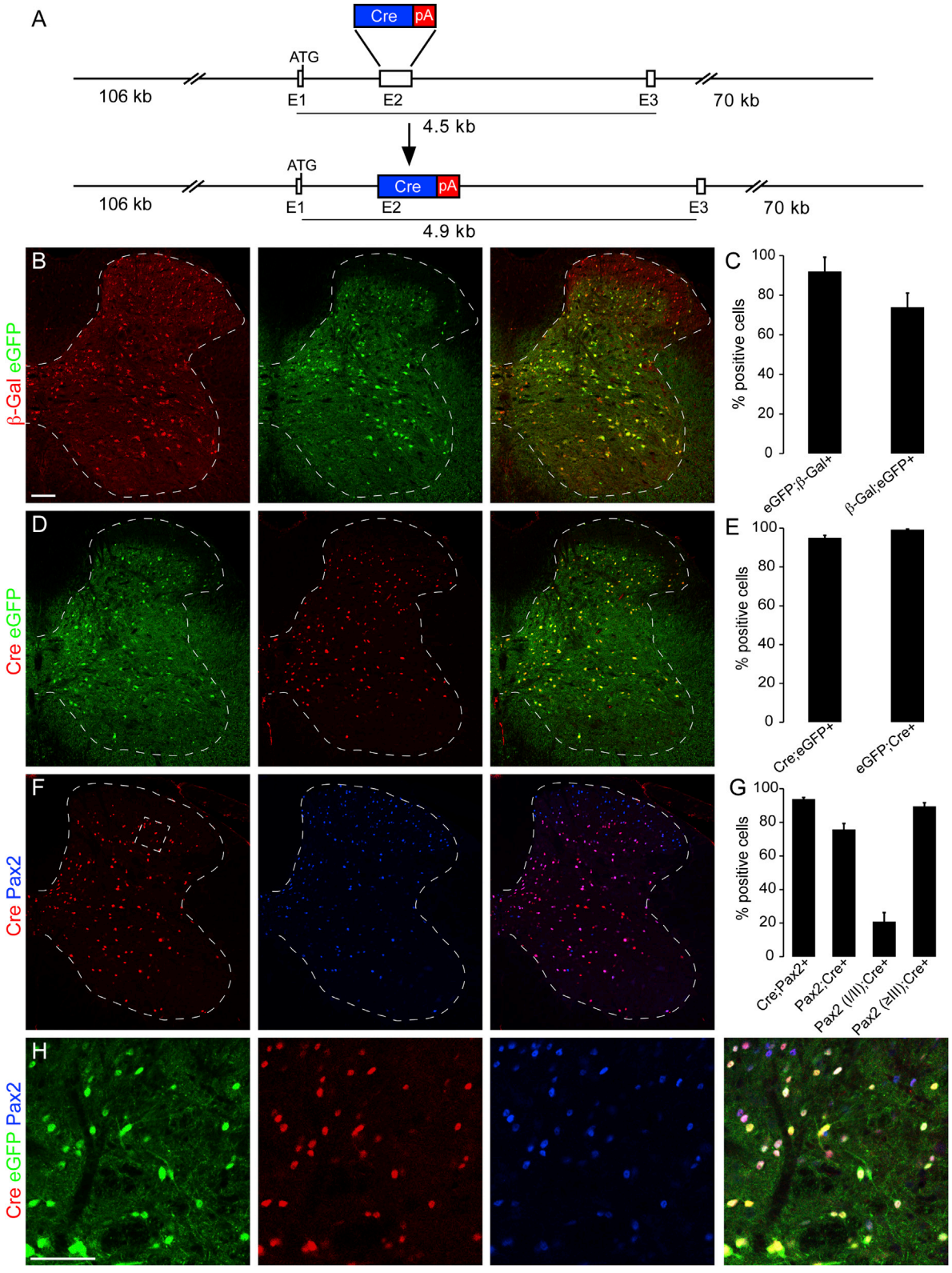

(legend on next page)

been hampered by the lack of appropriate molecular tools. Such studies became feasible with the advent of sophisticated viral vector-based approaches and Cre transgenic mouse lines. These technologies allow the functional and morphological mapping of neuronal circuits through retrograde tracing starting from precisely defined neuron populations (Wickersham et al., 2007) and the manipulation of specific subsets of neurons through ablation, silencing, and excitation in a spatially highly precise manner (Betley and Sternson, 2011).

To specifically address the role of the glycinergic neuron population in the dorsal horn, we generated a bacterial artificial chromosome (BAC) transgenic mouse line that expresses the Cre recombinase selectively in glycinergic neurons. Retrograde tracing experiments showed that glycinergic dorsal horn neurons receive sensory input mainly from low-threshold myelinated dorsal root ganglion (DRG) neurons. Local unilateral ablation of glycinergic neurons with diphtheria toxin or silencing of these neurons with tetanus toxin over three lumbar segments induced mechanical, heat, and cold hyperalgesia and signs of spontaneous aversive behavior, including extensive localized biting reminiscent of chronic itch. Accordingly, selective and local activation of glycinergic neurons alleviated nocifensive responses to acute noxious stimuli, hyperalgesia in neuropathic mice, and chloroquine- and histamine-induced itch responses.

RESULTS

Generation of GlyT2::Cre BAC Transgenic Mice

To specifically and locally manipulate glycinergic neurons, we generated a BAC transgenic mouse that expresses the Cre recombinase under the transcriptional control of the *GlyT2* gene, a marker of glycinergic neurons (Poyatos et al., 1997). We used the same strategy as employed previously for a GlyT2::eGFP BAC transgenic mouse (Zeilhofer et al., 2005; Figure 1A), whose eGFP expression pattern precisely recapitulated the distribution of glycinergic neurons (Hossaini et al., 2007; Zeilhofer et al., 2005). To characterize the spinal pattern of GlyT2::Cre-dependent recombination, we generated triple transgenic mice carrying the GlyT2::eGFP and GlyT2::Cre transgenes together with a *ROSA26*^{LacZ} reporter. We found a nearly complete match of β-galactosidase (β-gal) expression with GlyT2::eGFP in the deep dorsal horn, whereas the majority of superficial dorsal horn β-gal+ neurons lacked GlyT2::eGFP (Figures 1B and 1C). However, when the actual Cre protein expression pattern was analyzed in adult mice, an almost complete overlap of Cre and eGFP expression was found throughout the dorsal horn. Both were most abundant in the deep dorsal horn but largely absent from the superficial layers, suggesting that expression of the β-gal reporter in the superficial dorsal horn was caused by transient Cre expression during development (Figures 1D and 1E). To further confirm eutopic Cre expression, we demonstrate that nearly all (93.7% ± 1.5%) Cre+ neurons also stain positive for Pax2, a transcription factor expressed by more than 90% of adult spinal *Gad67*^{eGFP} and GlyT2::eGFP neurons (Figures 1F–1H; Figure S1). In the deep dorsal and ventral horn, almost 90% of Pax2+ neurons also expressed Cre, whereas this coexpression dropped to 20% in laminae I/II (Figures 1F–1H), which corresponds well with the spinal distribution of glycinergic neurons (Todd and Spike, 1993). The 20% Cre+ neurons of laminae I/II included most of the neuronal nitric oxide synthase (nNOS)+ inhibitory neurons in these laminae (Figure S2).

Primary Sensory Input onto Dorsal Horn Glycinergic Interneurons

The preferential localization of glycinergic neurons in the deep dorsal horn (i.e., in the termination areas of non-nociceptive primary sensory neurons) is consistent with what has been proposed in the gate control theory, but unequivocal proof for the innervation by non-nociceptive primary sensory neurons is lacking. Here we used a two-step rabies virus-based retrograde monosynaptic tracing strategy involving an EnvA pseudotyped eGFP rabies virus and TVA expression from a Cre-dependent adeno-associated virus (AAV) to map neurons presynaptic to dorsal horn glycinergic neurons (Figures 2A and 2B). Seven days after rabies virus injection, we found between 30 and 40 primary rabies virus-infected (TVA+/eGFP+) cells per spinal cord section (Figure S3) and numerous eGFP+ neurons in three to four adjacent lumbar DRGs ipsilateral to the virus injection site (Figure 2C), demonstrating the presence of direct synaptic input from primary sensory neurons onto glycinergic dorsal horn neurons. Ninety-one percent of these neurons (851 of 934) were myelinated (NF200+), including 7.6% (49 of 641) peptidergic (CGRP+/NF200+) neurons. Only 4.2% were NF200−/CGRP+ (27 of 641) and only 0.15% (1 of 664) were NF200+/IB4+ (Figures 2D–2F). These results are consistent with strong innervation of dorsal horn glycinergic neurons by non-nociceptive sensory neurons.

Figure 1. Generation and Characterization of GlyT2::Cre BAC Transgenic Mice

(A) GlyT2::Cre BAC transgenic mice were generated from a BAC DNA clone containing the mouse *GlyT2* locus, of which exon 2 (E2) was modified by the insertion of a Cre expression cassette.

(B) Comparison of Cre-mediated recombination and GlyT2::eGFP expression in GlyT2::Cre;GlyT2::eGFP;*Rosa26*^{LacZ} triple-transgenic mice using anti-β-gal (red) and anti-eGFP (green) antibodies.

(C) Percentage of β-gal and eGFP double-positive neurons (mean ± SD).

(D) Same as (B) but analysis of co-expression of Cre with eGFP.

(E) Quantification of (D).

(F) Same as (B) but analysis of co-expression of Cre with Pax2.

(G) Quantification of (F). The two left columns refer to the entire spinal cord cross section (laminae I–X), whereas the two right columns show results for the superficial dorsal horn (laminae I/II) and the rest of the spinal cord (≥III) separately.

(H) Higher magnification of the lamina II/III border (the dashed area indicated in F).

Scale bars, 100 μm (B) and 50 μm (F).

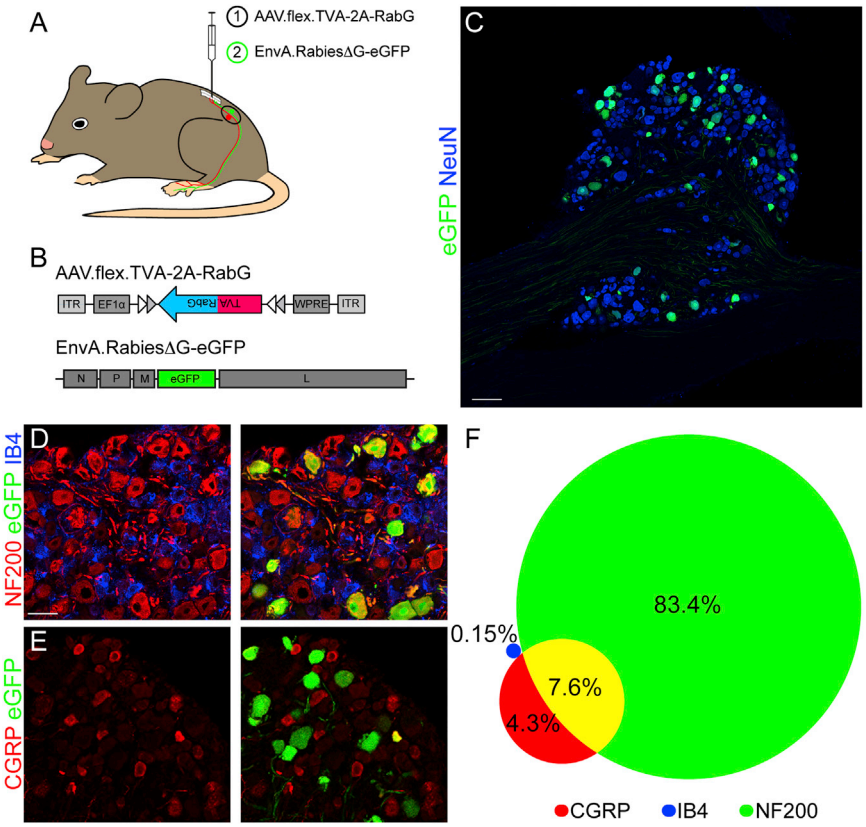

Figure 2. Innervation of Spinal Glycinergic Neurons by Primary Sensory Neurons

(A) Schematic of the injection paradigm enabling monosynaptic retrograde tracing from GlyT2::Cre+ spinal neurons. A Cre-dependent AAV coding for the avian sarcoma virus receptor and the rabies G protein (AAV.flex.TVA-2A-RabG, (1)) was injected 14 days prior to injection with an EnvA-pseudotyped G-deleted eGFP rabies virus (EnvA.RabiesΔG-eGFP, (2)).

(B) Schematic of the genomes of the AAV and rabies virus used in this experiment.

(C) A section of a DRG containing numerous retrogradely infected neurons was stained with antibodies against NeuN (blue) and eGFP (green).

(D and E) Immunohistological analysis of retrogradely infected DRG neurons. Shown are NF200 (red), eGFP (green), and IB4 (blue) (D) or antibodies against eGFP (green) and CGRP (red).

(F) Relative abundance of NF200+, CGRP+, or IB4+ cells among the eGFP+ (retrogradely infected) population of DRG neurons. Eight mice were analyzed.

Scale bars, 100 μm (C) and 50 μm (D).

Local Ablation of Dorsal Horn Glycinergic Neurons through AAV-Mediated Conditional Toxin Expression

To specifically and locally ablate spinal glycinergic neurons, we used intraspinal injections of serotype 1 AAV carrying a conditional (Cre-dependent) diphtheria toxin A fragment (DTA) expression cassette (AAV.flex.DTA; Figures 3A and 3B). Serotype 1 was chosen because retrograde infection of central neurons through axons or axon terminals by this serotype is generally negligible (Aschauer et al., 2013; Chamberlin et al., 1998). To ensure tight regulation of toxin expression, we used the FLEX system for irreversible Cre-dependent transgene activation (Atasoy et al., 2008; Figure 3B). We made three injections at lumbar segments L3/L4/L5 of 300 nl each at a depth of 200–300 μm from the dorsal surface of the spinal cord. To enable post hoc verification of the injected area, we added an eGFP reporter AAV to the injection solution. Infected (eGFP+) cells were confined to the injected side with a rostrocaudal spread of about 3-4 mm (Figure 3C). Loss of inhibitory (Pax2+) neurons was confined to a similar region of the ipsilateral spinal cord (Figure 3D). To assess the efficacy and specificity of this approach, we compared the numbers of inhibitory (Pax2+) and excitatory (Lmx1b+ and PKCγ+) dorsal horn neurons as well as of ventral horn (vesicular acetylcholine transporter [vAChT]+) motoneurons after AAV.flex.DTA injection in GlyT2::Cre+ and GlyT2::Cre− mice. Four days after intraspinal injection, the number of Pax2+ spinal neurons was reduced by 46.5% ± 4.0% in GlyT2::Cre+ mice relative to GlyT2::Cre− mice (one-way ANOVA, F(2,33) = 59.1, followed by Bonferroni post hoc test, $p < 0.001$) (Figures 3E and 3I). At day 26, the loss of inhibitory neurons was only slightly larger (59.9% ± 6.0%, $p = 0.15$). Ablation was most pronounced in laminae III/VI, where 65.4% ± 1.1% (one-way ANOVA, F(2,33) = 84.1, Bonferroni post hoc test, $p < 0.001$) of all inhibitory neurons were lost by day 4 (Figure 3I). Inhibitory interneuron loss in laminae I/II was less pronounced but still significant (17.5% ± 6.2% at day 4, one-way ANOVA, F(2,33) = 27.6, followed by Bonferroni post hoc test, $p < 0.001$). This is in good agreement with our observation that only about 20% of the superficial inhibitory neurons are GlyT2::Cre+ compared with more than 80% in the deep dorsal horn. No loss of excitatory dorsal horn neurons or motoneurons was detected (Figures 3F–3H and 3J–3L). This demonstrates not only that Cre-dependent ablation via AAV.flex.DTA was specific to glycinergic neurons but also rules out a secondary loss of neurons through excitotoxicity triggered by diminished inhibition.

Changes in Inhibitory Synaptic Transmission after Local Glycinergic Neuron Ablation

We next employed a combination of electrophysiology and optogenetics to quantify changes in inhibitory synaptic transmission onto laminae I/II neurons caused by glycinergic neuron ablation (Figure 4). We used horizontal spinal cord slices prepared from vGAT::ChR2-eYFP BAC transgenic mice (Zhao et al., 2011), which express an optimized channelrhodopsin (ChR-H134R) fused to a fluorescent reporter (eYFP) under the transcriptional control of the *vGAT* gene (i.e., in all inhibitory, GABAergic, and glycinergic neurons). For an electrophysiological characterization of light-induced action potential firing in dorsal horn glycinergic neurons and inhibitory synaptic transmission in these mice,

see Figure S4. We crossed vGAT::ChR2-eYFP mice with GlyT2::Cre+ mice to obtain GlyT2::Cre+;vGAT::ChR2-eYFP double transgenic and GlyT2::Cre-;vGAT::ChR2-eYFP control mice. Both strains underwent the same AAV.flex.DTA injections as for the morphological experiments (Figures 4Aa and 4Ab). Slices were prepared from the lumbar spinal cords 4 days after AAV.flex.DTA injection, and brief (4-ms) blue light stimuli were applied to evoke inhibitory postsynaptic currents (IPSCs). IPSCs were recorded from photocurrent-negative (i.e., presumed excitatory) neurons in the superficial dorsal horn (laminae I/II). In GlyT2::Cre-;vGAT::ChR2-eYFP mice, IPSCs had mean amplitudes of 1.39 ± 0.41 nA (n = 21), whereas those in GlyT2:Cre+;vGAT::ChR2-eYFP mice were only 0.62 ± 0.10 nA (n = 23) (Figures 4Ac and 4Ad). To test whether the remaining IPSCs originated from purely GABAergic neurons, we determined the relative contribution of glycine and GABA to the IPSC in GlyT2::Cre+ and GlyT2::Cre– mice after AAV.flex.DTA injection (Figure 4B). We found that, in both strains of mice, the glycine receptor antagonist strychnine blocked on average more than 70% of the total IPSC amplitude (73.0% ± 3.5%, n = 12, and 78.5% ± 3.9%, n = 15 for GlyT2::Cre– and GlyT2::Cre+ mice, respectively; $p < 0.05$, unpaired t test), whereas the remaining portion was blocked by the $GABA_A$ receptor antagonist bicuculline. Changing the order of strychnine/bicuculline application did not change the glycine/GABA ratio. These data indicate that most of the fast inhibitory synaptic input onto the recorded neurons came from mixed glycine/GABAergic neurons.

Local Ablation of Glycinergic Neurons Elicits Mechanical, Heat, and Cold Hypersensitivity and Signs of Spontaneous Pain

GlyT2::Cre+ mice exhibited hypersensitivity and spontaneous aversive behaviors as early as 24 hr after intraspinal injection with AAV.flex.DTA (Figure 5). To characterize this phenotype quantitatively, we assessed GlyT2::Cre+ and GlyT2::Cre– littermates in a battery of behavioral tests. In the von Frey test for mechanical sensitization, GlyT2::Cre+ mice showed a significant reduction in paw withdrawal thresholds (PWTs), whereas no change was observed in GlyT2::Cre– mice (Figure 5A; for statistics, see figure legend). From day 2 post-injection onward, PWTs of GlyT2::Cre+ mice were reduced significantly compared with the baseline (repeated measures ANOVA, $F(13,130) = 17.5$; least significant difference (LSD) post hoc test, $p < 0.01$), reaching a minimum 5 days after virus injection. From day 13 onward, PWTs recovered significantly toward the baseline (LSD post hoc test, $p < 0.01$ for day 5 versus day 13 or later), suggesting the presence of compensatory processes. A similar sensitization process was observed for heat and noxious cold stimuli (Figures 5B and 5C). Nociceptive thresholds for contralateral paws of both GlyT2::Cre+ or GlyT2::Cre– mice remained virtually unchanged for all three stimuli (Figures S5A–S5C; for statistics, see figure legends).

Inhibitory neurons also play an important role in ventral motor circuits. To demonstrate that targeting of glycinergic interneurons did not cause confounding motor impairment, we assessed motor performance on an accelerating rotarod. GlyT2::Cre+ mice showed a slight progressive decrease in the maximum tolerated speed over 25 days (Figure 5D), but this did not match the time course of neuronal death or hyperalgesia.

In addition to hyperalgesia, we also observed signs of spontaneous discomfort that included flinching, licking/biting, and limb guarding/protection of the ipsilateral hindlimb. From 3–4 days post-injection, localized hair loss and skin lesions became apparent on the virus-injected side (Figure 5E). In the majority of cases, the area of hair removal extended along the thigh, closely matching the dermatomes corresponding to the AAV.flex.DTA-injected spinal segments. The contralateral side showed no evidence of hypersensitivity or hair loss and lesions. Similarly, AAV.flex.DTA-injected GlyT2::Cre– mice remained completely normal. To assess spontaneous aversive behaviors, we quantified paw flinches in AAV.flex.DTA-injected mice and the time the animals spent licking/biting the affected limb. In GlyT2::Cre+ mice, we observed a significant increase in flinching and the time spent licking/biting, which peaked around 4 days after injection (Figure 5F). After day 4, the frequency of flinching decreased over the course of the remaining experiment, mirroring the recovery from thermal and mechanical hyperalgesia.

We next investigated the expression of c-*fos*, a marker of neuronal activation, in AAV.flex.DTA-injected mice as an additional non-behavioral readout. We harvested the spinal cords 24 hr after the last day of behavioral testing and immunostained horizontal sections of the virus-injected segments. The number of c-*fos*+ somata was significantly increased in GlyT2::Cre+ mice compared with GlyT2::Cre– mice (Figure 5G). The c-*fos*+ neurons were evenly distributed within laminae I–IV, and a few positive somata were located in laminae V and VI. We observed few c-*fos*+ neurons on the contralateral side or in sections from GlyT2::Cre– mice. A large increase in the number of labeled soma was seen after 4 days (76.6 ± 37 in Cre+ versus 10.8 ± 5.4 in Cre– mice). By the end of the experiment, the number of c-*fos*+ neurons had decreased (19.1 ± 9 in Cre+ versus 1.6 ± 1.4 in Cre– mice). The changes in c-*fos* expression therefore mirrored the results of the behavioral experiments.

Tetanus Toxin-Mediated Synaptic Silencing Recapitulates Behavioral Effects of Cell Ablation

Viral infection and neuronal cell death activate microglia. An upregulation of the microglia marker IBA1 was indeed observed following ablation of glycinergic neurons with AAV.flex.DTA (Figure S6). It has been shown previously that activation of dorsal horn microglia alone is sufficient to cause pain sensitization (Clark et al., 2007; Coyle, 1998; Tanga et al., 2004). We therefore generated a second AAV (AAV.flex.TeLC) for Cre-dependent expression of tetanus toxin light chain (TeLC), which silences neurons by preventing vesicular transmitter release (Sweeney et al., 1995). As expected, dorsal horn injection of AAV.flex.TeLC did not cause loss of spinal neurons (Figures 6A–6H), and no difference in IBA1 expression was observed between GlyT2::Cre+ and GlyT2::Cre– mice after AAV.flex.TeLC injection (Figure S6). Following AAV.flex.TeLC injection, GlyT2::Cre+ mice developed strong mechanical, heat, and noxious cold sensitization and exhibited localized hair loss and lesions (see legend for Figure 7 for statistics). They also showed a significant increase in flinching and licking/biting behavior (Figures 7A–7E). Sensitization began

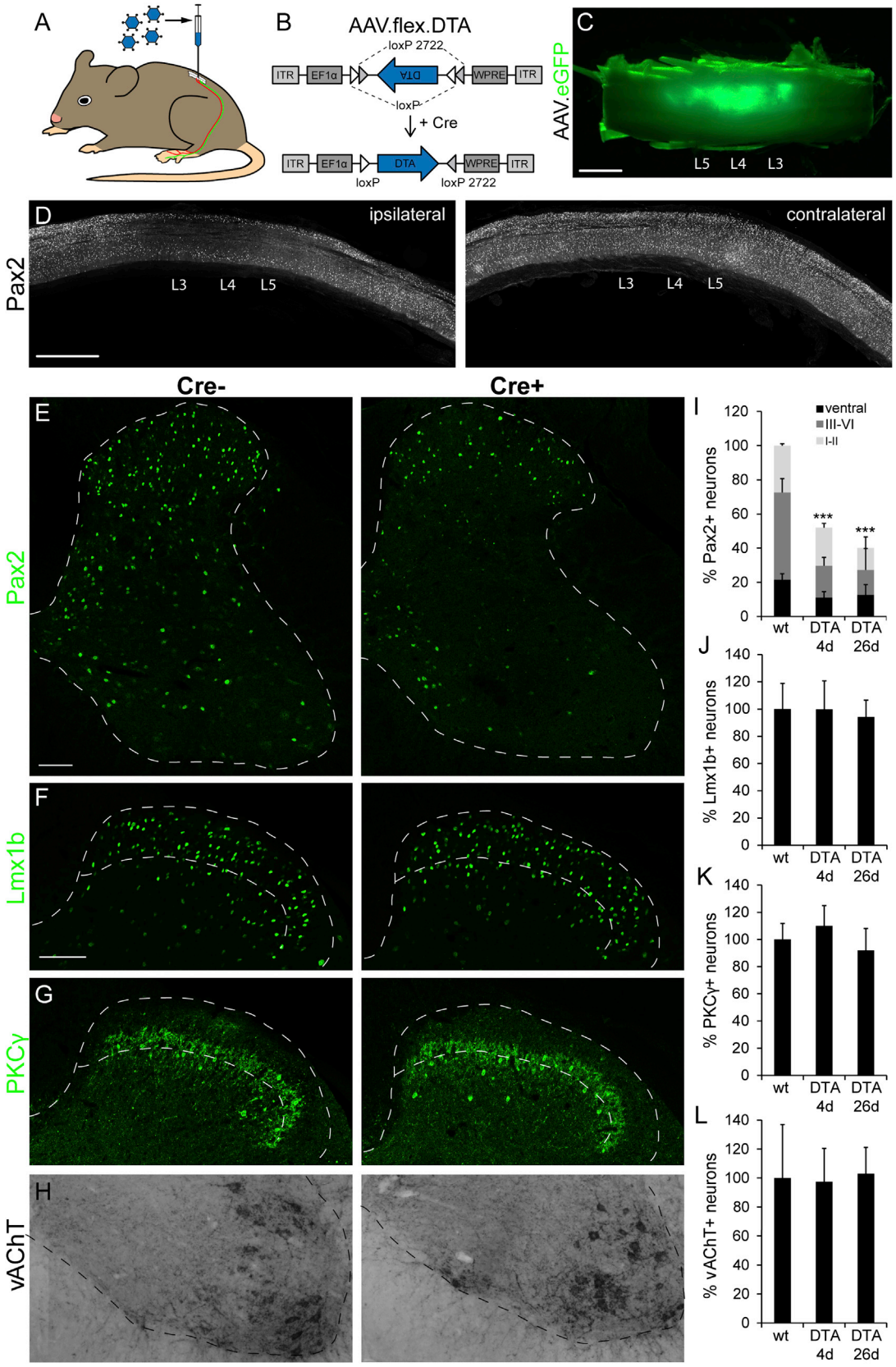

(legend on next page)

to decrease from day 10 onward. We also found a significant increase in the number of c-*fos*+ cells 4 days and 26 days after injection of AAV.flex.TeLC (Figure 7F). No changes were seen in the contralateral paw (Figure S5). The results obtained with tetanus toxin-mediated silencing therefore closely mirrored the effects of AAV.flex.DTA-mediated cell ablation.

Local Pharmacogenetic Activation of Dorsal Horn Glycinergic Neurons Mitigates Neuropathic Hyperalgesia

Our observation that glycinergic neurons serve a critical role in maintaining a physiological level of pain sensitivity prompted us to test whether exogenous activation of glycinergic neurons ameliorates chronic pain. To this end, we employed a pharmacogenetic approach (Armbruster et al., 2007) and injected GlyT2::Cre;GlyT2::eGFP double-transgenic mice with AAV.flex.hM3Dq-mCherry, targeted to the left L3–L5 spinal segments. AAV.flex.hM3Dq encodes an engineered G protein-coupled receptor that renders Cre-expressing neurons responsive to activation by clozapine N-oxide (CNO) (Alexander et al., 2009; Figure 8A). We verified expression of hM3Dq-mCherry in the somata and neurites of GlyT2::eGFP+ neurons 2 weeks post-injection (Figure 8B). Transduced neurons were largely confined to lamina III/VI of the dorsal horn. No mCherry+ cell bodies were found in the ipsilateral ventral horn or on the contralateral side.

One week after virus injection, a unilateral neuropathic sensitization of the hindpaw ipsilateral to the side of virus injection was induced through a chronic constriction injury (CCI) of the sciatic nerve (Bennett and Xie, 1988). On day 7 after CCI surgery, we injected CNO (1 mg/kg, i.p.]) or vehicle and assessed mechanical (von Frey) paw withdrawal thresholds for 5 hr. Within 1-2 hr after CNO administration, mechanical sensitivity decreased significantly in drug-treated but not vehicle-treated GlyT2::Cre+ mice (Figure 8C). Vehicle-injected mice showed no improvement over the testing period. We also tested whether activation of glycinergic neurons would reduce responses to acute noxious stimuli (Figure 8D). CNO prolonged withdrawal latencies upon heat and noxious cold stimulation more than 2-fold in naive AAV.flex.hM3Dq-injected GlyT2::Cre mice. Similarly, CNO reduced the number of escape responses upon pinprick stimulation of the hindpaw. To exclude muscle relaxation as a confounder, we assessed the performance of CNO and vehicle-injected CCI mice in the horizontal wire test and found no difference (Figure 8E). Taken together, these results demonstrate that activation of dorsal horn glycinergic neurons effectively alleviates neuropathic hyperalgesia.

Dorsal Horn Glycinergic Neurons Control Histamine- or Chloroquine-Induced Itch

GlyT2::Cre+ mice injected with AAV.flex.DTA or AAV.flex.TeLC not only developed long-lasting thermal and mechanical hypersensitivity but also displayed excessive localized licking and biting behavior leading to hair removal and skin lesions. This behavior is reminiscent of changes typically seen with chronic itch (Akiyama and Carstens, 2013; Ross et al., 2010). We therefore tested whether mice would respond more strongly to pruritic stimuli after local spinal ablation of glycinergic neurons. These experiments did not yield conclusive results, probably because the spontaneous aversive behavior was too intense to detect further increases. As an alternative strategy, we examined whether pharmacogenetic activation of spinal glycinergic neurons would attenuate responses to puritic stimuli. To this end, we again injected GlyT2::Cre+ mice with AAV.flex.hM3Dq-mCherry. Two weeks after virus injection, their ipsilateral hindpaws were injected intracutaneously with either chloroquine or histamine (Figure 8F). Compared with vehicle, CNO significantly reduced the number of flinching and biting bouts induced by the injection of histamine or chloroquine. This final set of experiments indicates that spinal glycinergic neurons control not only pain but also itch transmission.

DISCUSSION

In this study, we used viral vector-mediated neuron manipulation to address a possible contribution of local glycinergic dorsal horn neurons to pain and itch control. The results from the comprehensive set of experiments involving local ablation or silencing of these neurons demonstrate that compromising their function induces an exaggerated abnormal sensitivity to mechanical, heat, and cold stimuli and triggers behavioral changes reminiscent of spontaneous pain and itch. Conversely, pharmacogenetic excitation of the same neurons alleviated neuropathic pain and itch.

Figure 3. Specific Loss of Inhibitory Interneurons after AAV.flex.DTA Injection into the Dorsal Horn of GlyT2::Cre+ Mice

(A) AAV.flex.DTA was injected into the lumbar dorsal horn of GlyT2::Cre+ GlyT2::Cre− littermates.

(B) The AAV.flex.DTA genome. The expression of DTA is driven by the EF1a promotor (EF1a) and depends on Cre-mediated irreversible inversion of the DTA coding sequence.

(C) Green fluorescence illustrates virus spread (of an AAV.eGFP) following three separate unilateral injections into the lumbar spinal cord at levels L3–L5.

(D) Sagittal sections of a spinal cord after injection of AAV.flex.DTA illustrate a marked reduction in the number of Pax2+ cells on the ipsilateral side (left) but not on the contralateral side (right).

(E) Compared with AAV.flex.DTA-injected GlyT2::Cre− control mice, a clear loss of Pax2+ cells was observed 4 days after injection of AAV.flex.DTA on the injected side of GlyT2::Cre+ mice. Fluorescence signals detected by confocal microscopy were false-colored in green.

(F–H) Same as (E) but analysis of Lmx1b+ excitatory dorsal horn neurons (F), PKCγ+ excitatory dorsal horn neurons (G), and vAChT+ motoneurons (H).

(I–L) Quantification (mean ± SD). At least three to four horizontal sections per mouse centered around the L4 injection site were used for quantification.

(I) ***$p < 0.001$ versus baseline, one-way ANOVA, $F(2,33) = 59.1$, followed by Bonferroni post hoc test.

(I–K) No significant differences in cell counts were found for Lmx1b+, PKCγ+, or vAChT+ neurons ($p > 0.20$). Dashed lines indicate gray matter border (E–H) and borders of lamina II (F and G).

Scale bars, 1 mm (C and D) and 100 μm (E and H).

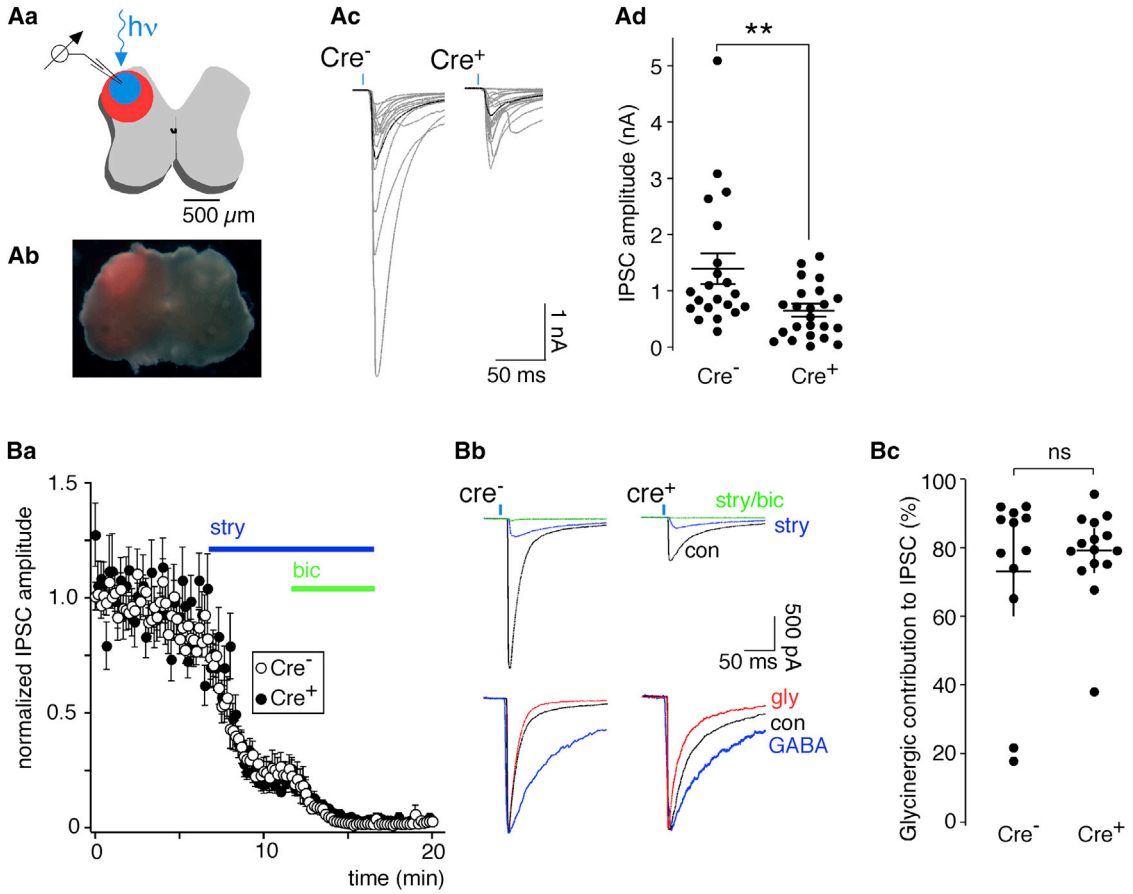

Figure 4. Inhibitory Synaptic Transmission after Local Glycinergic Interneuron Ablation

(Aa–Ad) IPSCs evoked by 4-ms, 473-nm light stimulation recorded in slices prepared from mice 4 days after AAV.flex.DTA injection.

(Aa) Schematic illustrating the recording situation.

(Ab) Distribution of mCherry expression observed after unilateral injection of AAV.mCherry together with the AAV.flex.DTA.

(Ac) Average IPSC traces per cell (gray) of 21 neurons from GlyT2::Cre− (left) and 23 neurons from GlyT2::Cre+ mice (right). Black traces represent the average IPSC for each genotype.

(Ad) Statistics. Dots represent average IPSC amplitudes of individual cells. Horizontal and vertical lines indicate mean values and SEM. $^{**}p < 0.01$ (unpaired t test).

(Ba–Bc) Contribution of glycine and GABA to the IPSC amplitude in AAV.flex.DTA-injected GlyT2::Cre+ and GlyT2::Cre− mice.

(Ba) Time course of the experiment. Strychnine (stry, 0.5 μM) and a combination of strychnine (0.5 μM) and bicuculline (bic, 20 μM) were applied 6 and 12 min after the recording started.

(Bb) The top traces show averages of 10 consecutive traces recorded under control conditions during application of strychnine and in the combined presence of strychnine and bicuculline. The normalized traces below illustrate the difference in the decay kinetics of the GABAergic and glycinergic IPSC components.

(Bc) Statistics. Dots represent the glycinergic IPSC component in individual cells. Horizontal and vertical lines indicate mean values and SEM, $p = 0.49$ (unpaired t test), $n = 12$ and 15 for GlyT2::Cre- and GlyT2::Cre+ mice, respectively.

Vector-Mediated Ablation as a Tool of Interneuron Manipulation

Clostridial toxins are highly versatile tools to manipulate cell function. In this study, we used the catalytic subunits of diphtheria toxin or tetanus toxin to locally ablate or silence glycinergic neurons. Cell-type-specific manipulation through diphtheria toxin or tetanus toxin can be achieved through different strategies. Expression as Cre-dependent germline transgenes is well established (Palmiter et al., 1987) but would have led to global ablation of glycinergic neurons early in development and likely to subsequent early death (Gomeza et al., 2003). Buch et al. (2005) introduced a method for inducible cell-type-specific ablation involving Cre-dependent expression of the diphtheria toxin receptor followed by local injection of diphtheria toxin. However, because GlyT2::Cre is transiently active in superficial dorsal horn neurons that are not glycinergic in the adult, this approach would still have lacked specificity. To circumvent these problems, we chose the viral approach, which enables local manipulation and avoids undesired effects originating from transient Cre expression during development.

Glycine Is the Dominant Inhibitory Neurotransmitter in Pain- and Itch-Controlling Spinal Circuits

Glycinergic neurons of the spinal dorsal horn are most abundant in lamina III and deeper, whereas only relatively few glycinergic neurons are found in the superficial layers (lamina I/II)

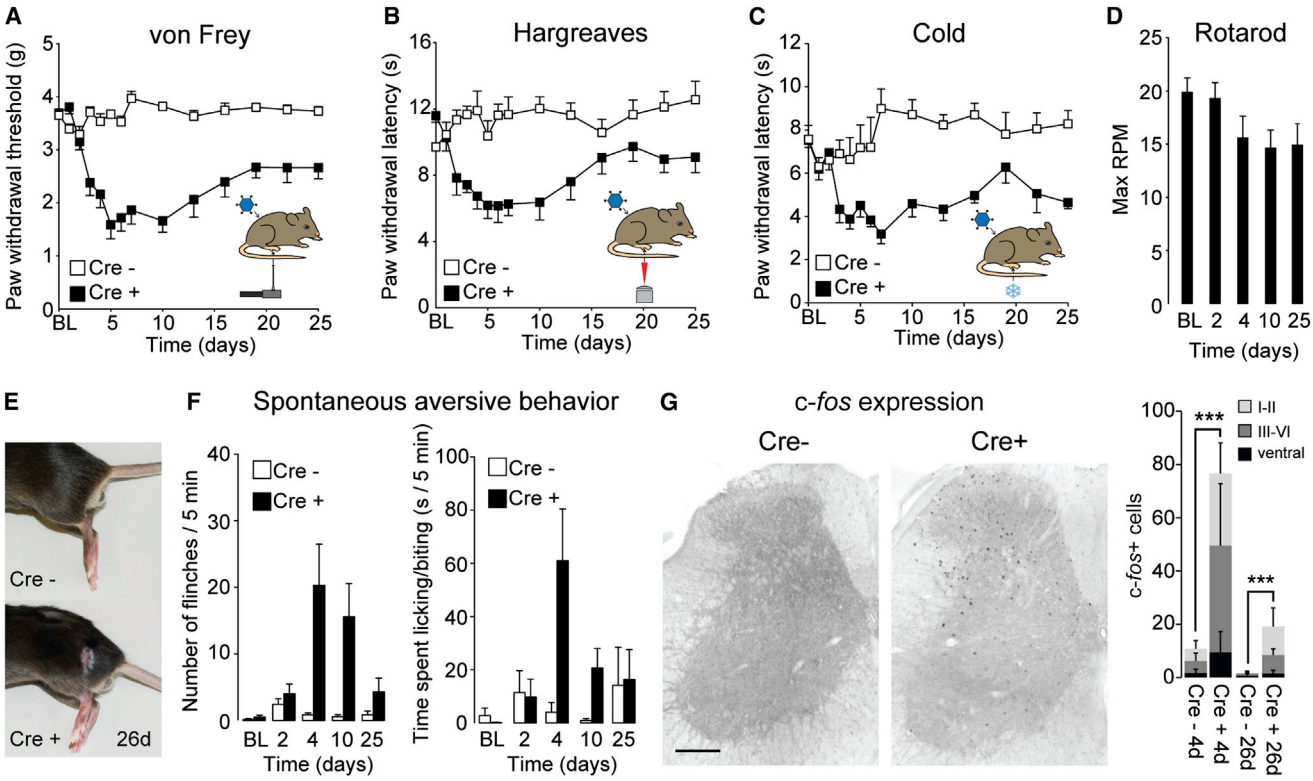

Figure 5. Mechanical, Heat, and Cold Hyperalgesia and Spontaneous Aversive Behaviors Induced after Local Ablation of Glycinergic Dorsal Horn Neurons

(A) Reduction in mechanical PWT (mean ± SEM) over time after unilateral injection of AAV.flex.DTA into GlyT2::Cre+ mice and GlyT2::Cre− littermates. Two-way repeated measures ANOVA revealed a significant time x genotype interaction ($F(13,221) = 13.9$, $p < 0.001$), and post hoc comparisons show significant differences between genotypes at 3–25 days ($p < 0.01$, n = 11 and 8 for GlyT2::Cre+ and GlyT2::Cre− mice, respectively). baseline.

(B) Heat hyperalgesia. Two-way repeated measures ANOVA revealed a significant time x genotype interaction ($F(13,221) = 4.04$, $p < 0.001$). Significant differences between genotypes were found for time points 3–10 days ($p < 0.01$, n = 11 and 8 for GlyT2::Cre+ and GlyT2::Cre− mice, respectively).

(C) Cold hyperalgesia. Two-way repeated measures ANOVA revealed a significant time x genotype interaction ($F(13,143) = 2.81$, $p = 0.001$). Significant differences were found between genotypes for time points 7–16 days ($p < 0.01$, n = 6 and 7 for GlyT2::Cre+ and GlyT2::Cre− mice, respectively).

(D) Accelerating rotarod performance (maximum tolerated rounds per minute [RPM]). Repeated measures ANOVA, $F(4,40) = 4.14$; $p = 0.007$ (n = 11). Post hoc LSD test revealed a significant change from the baseline for day 25 only.

(E) GlyT2::Cre+ mice, but not GlyT2::Cre− littermates, exhibited localized hair loss on the thigh ipsilateral to the virus injection (depicted here 26 days after virus injection).

(F) Spontaneous aversive behaviors (flinches, left, and time spent licking/biting, right) in GlyT2::Cre+ mice and GlyT2::Cre− littermates (n = 7 each). Two-way repeated measures ANOVA revealed a significant time x genotype interaction for flinching ($F(4,48) = 7.02$, $p < 0.001$), and time spent licking/biting ($F(4,48) = 7.02$, $p < 0.001$). Significant differences between genotypes were found for days 4 and 10 ($p \leq 0.01$ for both readouts). On day 25, the number of flinches and the time spent licking/biting were reduced significantly compared with day 4 ($p < 0.05$).

(G) c-*fos* expression in spinal cords of GlyT2::Cre+ mice and GlyT2::Cre− littermates 4 days after dorsal horn AAV.flex.DTA injection. ***$p < 0.001$, unpaired t test, n ≥ 9 sections from 3-4 different animals. Scale bar, 200 μm.

Error bars indicate SEM in (A–D) and (F) and SD in (G).

(Hossaini et al., 2007; Polgár et al., 2013; Todd and Spike, 1993; Zeilhofer et al., 2005). They are therefore relatively sparse in the laminae innervated by primary nociceptive fibers and much more frequent in the deep dorsal horn, where mainly non-nociceptive mechanosensitive fibers terminate. Indeed, our results demonstrated strong innervation by myelinated presumed non-nociceptive neurons (Figure 2). The concentration of glycinergic neurons in the deep dorsal horn has led to the suggestion that their dysfunction might primarily induce touch-evoked pain (also known as allodynia) (Lu et al., 2013; Miraucourt et al., 2009). Our results also point to a critical role of glycinergic neurons in the processing of noxious thermal and mechanical input. Such a more general role in pain control is consistent with the results from our optogenetic experiments, which demonstrate that most of the inhibitory input onto superficial dorsal horn neurons is glycinergic (see also Keller et al., 2001). The presence of strong glycinergic inhibition in the superficial dorsal horn is also consistent with a dense expression of glycine receptors of the α3 subtype at this site (Harvey et al., 2004) and the abundance of GlyT2-positive neuropil (Zeilhofer et al., 2005). In fact, it has been shown recently that positive allosteric modulators of dorsal horn glycine

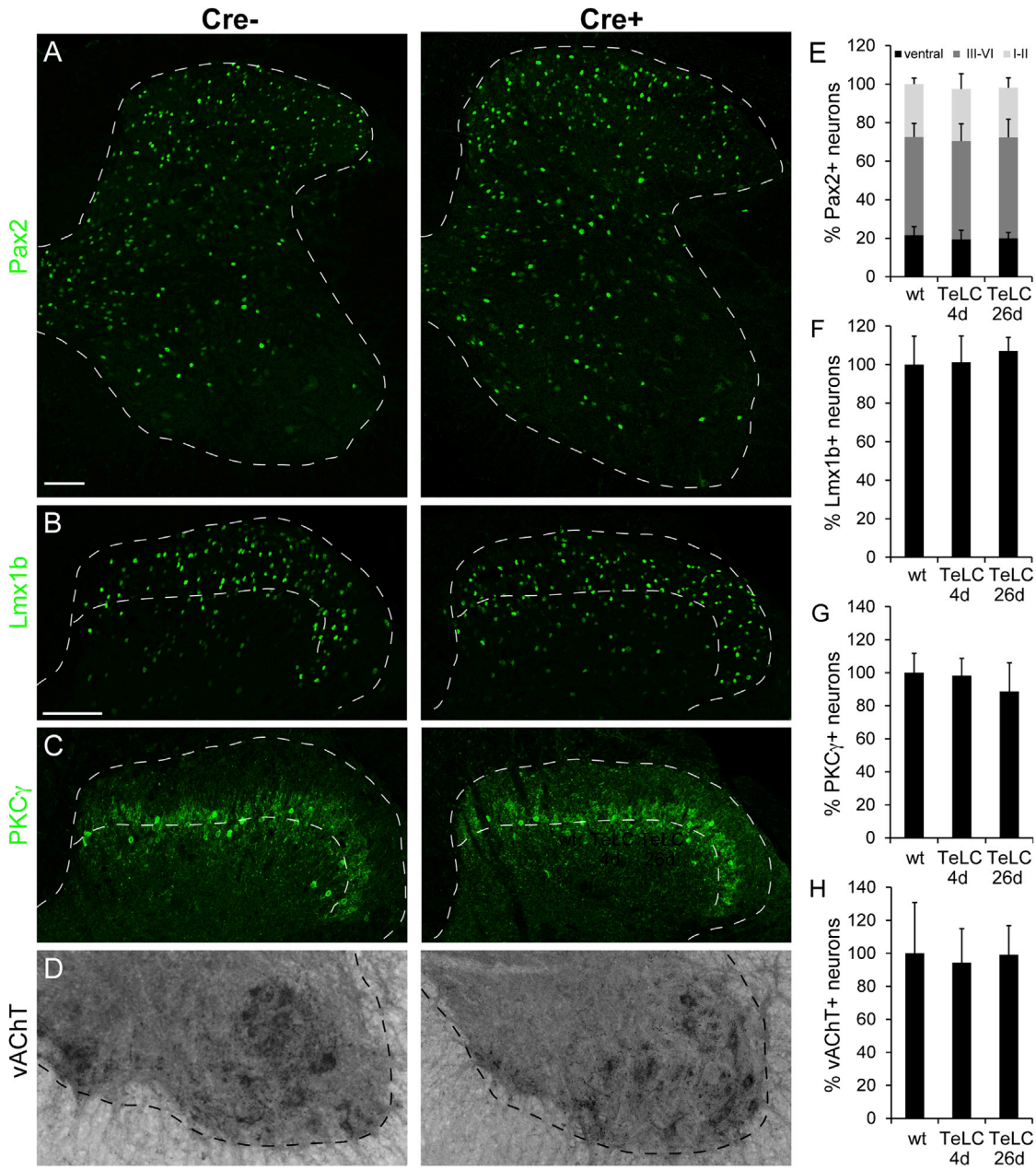

Figure 6. Expression of Tetanus Toxin Light Chain in Glycinergic Dorsal Horn Interneurons Does Not Cause Neuronal Death

(A) No loss of Pax2 immunoreactive cells following AAV.flex.TeLC injection into GlyT2::Cre+ mice (images taken 4 days after virus injection).

(B–D) No apparent loss of Lmx1b+ excitatory dorsal horn neurons (B), of PKCγ+ excitatory dorsal horn neurons (C), or of vAChT+ motoneurons (D) was detected.

(E–H) Quantifications (percent relative to GlyT2::Cre−, mean ± SD). Scale bars, 100 μm (A and B).

receptors effectively reverse pathological pain states (Lu et al., 2013; Xiong et al., 2011, 2012).

Activation of Spinal Glycinergic Neurons Effectively Alleviates Neuropathic Pain

Chronic pain is accompanied by states of diminished synaptic inhibition of dorsal horn neurons. This disinhibition is widely believed to contribute to pain hypersensitivity and to spontaneous pain sensations (Zeilhofer et al., 2012). A variety of different mechanisms, including reduced expression of the GABA synthesizing enzyme GAD-65 (Moore et al., 2002; Scholz et al., 2005), reduced release of GABA and/or glycine (Müller et al., 2003) and reduced responsiveness of postsynaptic glycine receptors (Ahmadi et al., 2002; Harvey et al., 2004), have been proposed as mechanisms of diminished inhibition. Our finding that glycinergic neuron ablation or silencing induces thermal

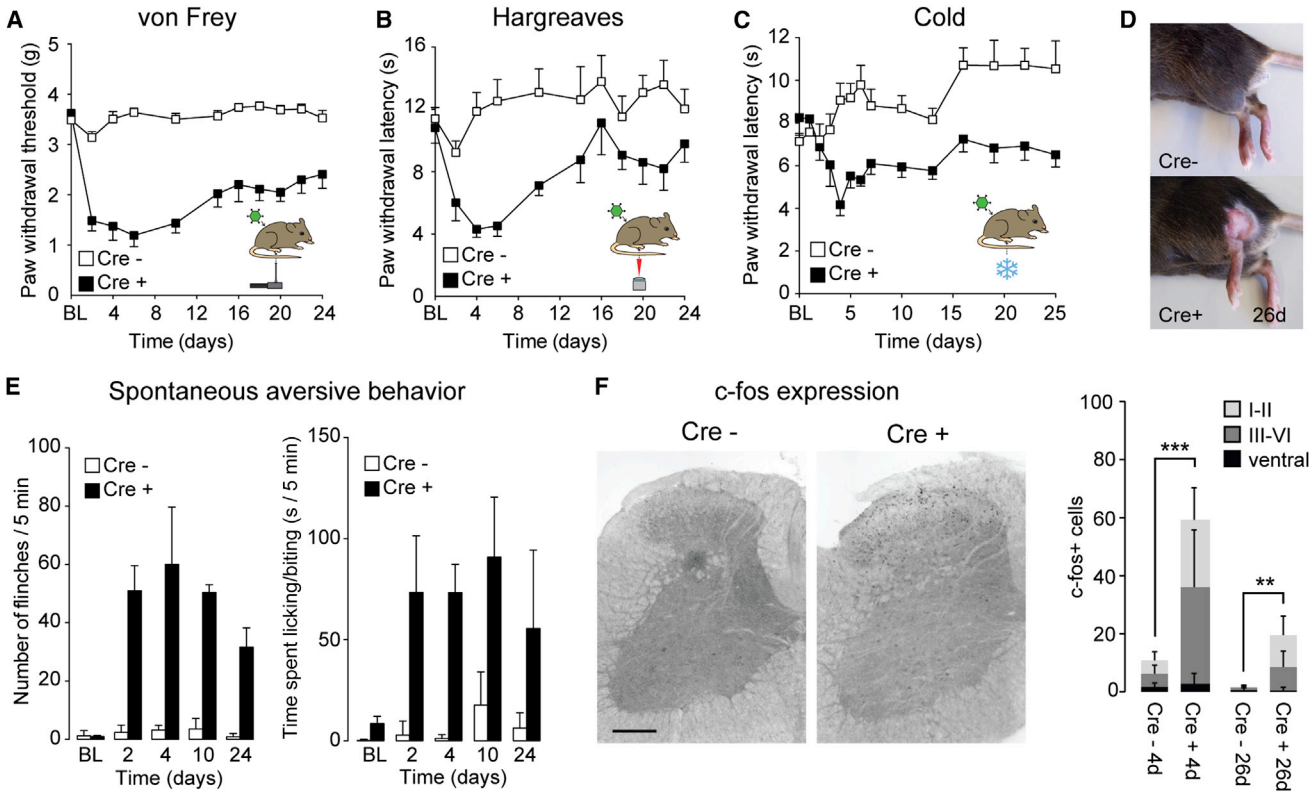

Figure 7. Local Silencing with Tetanus Toxin Light Chain of Glycinergic Dorsal Horn Neurons Recapitulates the Behavioral Effects of Diphtheria Toxin-Mediated Ablation

(A) Mechanical hyperalgesia. Statistics: significant time x genotype interaction, $F(10,140) = 12.4$, $p < 0.001$ (two-way repeated measures ANOVA). Post hoc comparisons show significant differences between genotypes at 2–24 days ($p < 0.01$, $n = 8$ for both genotypes).

(B) Heat hyperalgesia: significant time x genotype interaction ($F(10,140) = 42.35$, $p < 0.05$). Significant differences between genotypes were found for time points 4–10 days ($p < 0.01$, $n = 8$ for both genotypes).

(C) Same as (B) but cold hyperalgesia. Repeated measures ANOVA ($F(13,247) = 4.0$, $p < 0.001$). Significant differences between genotypes were found ($p \leq 0.01$) for time points 4–16 days ($n = 10$ and 11 for GlyT2::Cre+ and GlyT2::Cre− mice, respectively).

(D) Localized hair removal and skin lesions (26 days after AAV.flex.TeLC injection).

(E) Spontaneous aversive behaviors ($n = 5$ and 6 for GlyT2::Cre+ and Cre− mice, respectively). ANOVA revealed significant differences for between subject effect (genotype) ($F(1,9) = 48.3$, $p < 0.001$ and $F(1,9) = 76.3$ $p < 0.001$ for flinching and licking/biting, respectively).

(F) c-*fos* expression (images taken 4 days after AAV.flex.TeLC injection). ***$p < 0.001$; **$p < 0.01$, unpaired t test comparing the total number of c-*fos*+ cells from all laminae, $n = 4–7$.

For more details, see Figure 5. Error bars indicate SEM in (A–C) and (E) and SD in (F). Scale bar, 200 μm.

and mechanical sensitization and spontaneous pain behaviors is fully in line with this concept. Another process linking peripheral nerve damage to reduced inhibition in the dorsal horn is the microglia-mediated and brain-derived neurotrophic factor-dependent downregulation of the potassium-chloride co-exporter KCC2 (Coull et al., 2003, 2005). Reduced expression of this transporter causes a depolarizing shift of the reversal potential of glycinergic and GABAergic currents. It has been proposed that this shift may even reach the threshold of action potentials and would, thereby, change the effect of GABAergic and glycinergic input from inhibition to excitation (Coull et al., 2003). Our experiments employing pharmacogenetic activation of local glycinergic neurons suggest that these neurons retain their inhibitory action even in the presence of neuropathy. This result is consistent with the reversal of neuropathic pain sensitization by drugs that potentiate the activation of $GABA_A$ receptors in the dorsal horn (Knabl et al., 2008) and by transplantation of GABAergic precursor neurons into the dorsal horn of neuropathic mice (Bráz et al., 2012).

Contribution of Neuronal Death or Virus-Activated Microglia?

Neuronal cell death is a strong activator of microglia. It was therefore important to investigate whether diphtheria toxin-induced cell death would activate microglia and whether this microglia activation would, in turn, contribute to pain sensitization. Quantification of IBA1 immunoreactivity in AAV.flex.DTA-injected dorsal horns demonstrated strong microglia activation in GlyT2::Cre+ mice and, to a much lesser degree, in GlyT2::Cre– mice. However, AAV.flex.DTA-mediated neuronal death and AAV.flex.TeLC-mediated silencing of the same neuron types led to virtually identical pain phenotypes despite strong

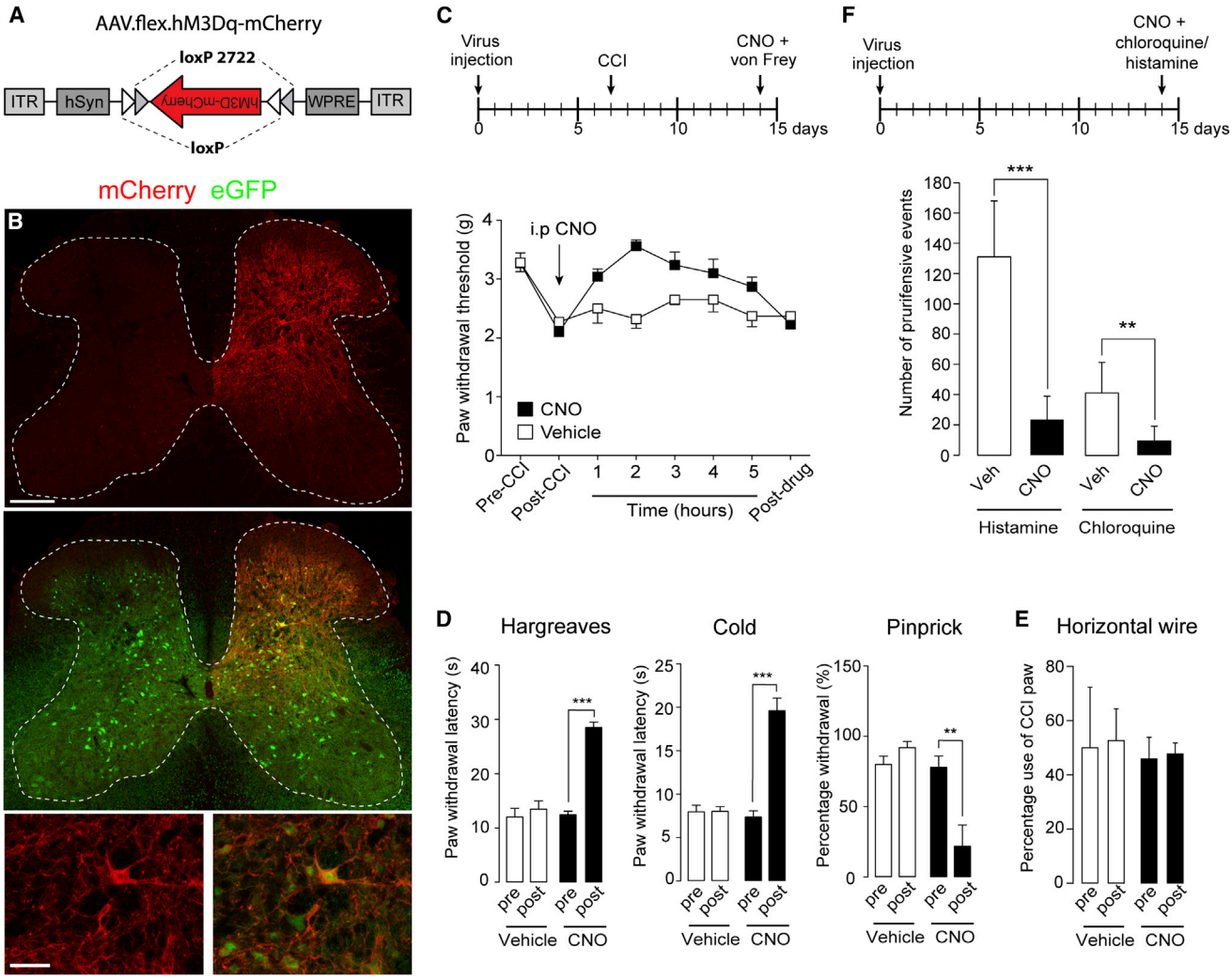

Figure 8. Pharmacogenetic Activation of Spinal Glycinergic Neurons Ameliorates CCI-Induced Neuropathic Pain and Chloroquine- or Histamine-Induced Itch

(A) Diagram illustrating the AAV genome containing the flex.hM3Dq-mCherry cassette.

(B) Expression of hM3Dq in the spinal cord of GlyT2::Cre;GlyT2::eGFP double-transgenic mice is indicated by mCherry fluorescence. Expression is limited to the ipsilateral dorsal horn and is present in somata (see detail, bottom) and neurites of eGFP+ neurons. Scale bars, 200 μm (top) and 50 μm (bottom).

(C) Antihyperalgesic effects. All experiments were made in GlyT2::Cre+ mice. AAV.flex.hM3Dq-mCherry was injected at day 0, CCI surgery was performed on day 7 on virus-injected mice, and vehicle or CNO (1 mg/kg, i.p.) was injected on day 14. Mechanical PWTs (g) were assessed using electronic von Frey filaments before CCI surgery (pre-CCI), after CCI surgery immediately before CNO/vehicle injection (post-CCI), for 5 hr after CNO/vehicle injection, and 1 day later (post-drug). Repeated measures ANOVA, $F(6,66) = 4.47$; $p = 0.001$ for treatment x time interaction. Post hoc comparisons revealed significant differences between CNO and vehicle-treated groups for time points 2 and 3 hr (n = 6 and 7 for vehicle and CNO, respectively).

(D) Acute antinociceptive effects (repeated-measures ANOVA). Significant treatment effects were observed in the Hargreaves test ($F(1,9) = 43.1$, $p < 0.001$ [n = 5 and 6 for CNO and vehicle, respectively]), for cold hyperalgesia ($F(1,9) = 56.2$, $p < 0.001$ [n = 6 and 5]), and for pinprick stimulation ($F(1,8) = 21.0$, $p = 0.002$ [n = 5 each]).

(E) Horizontal wire test. Repeated measures ANOVA ($F(1,7) = 0.001$, $p = 0.98$).

(F) Blockade of chloroquine- and histamine-induced itch in AAV.flex.hM3Dq-mCherry-injected GlyT2::Cre+ mice by CNO. ***$p < 0.001$; **$p < 0.01$, unpaired t test, n = 7 for all four groups.

All error bars indicate SEM.

differences in the degree of IBA1 upregulation. Hence, the pain was due to the ablation or silencing of glycinergic neurons rather than due to secondary microglia activation. Microinjections into the spinal cord are alone sufficient to induce microglia activation (Hutson et al., 2012). We found similar degrees of microglial IBA1 upregulation in AAV.flex.TeLC-injected GlyT2::Cre– and GlyT2::Cre+ mice. However, pain sensitization occurred only in GlyT2::Cre+ mice; i.e., under conditions in which the glycinergic neurons were silenced. Pain sensitization by microglia may therefore require a specific microglial

activation state (Graeber and Christie, 2012; Hanisch and Kettenmann, 2007; Taves et al., 2013).

Spinal Plasticity Ameliorating Long-Lasting Pain?

An unexpected finding in our behavioral experiments was the partial recovery from pain sensitization after glycinergic neuron ablation or silencing. The results discussed above largely rule out recovery from microglia-induced pain sensitization as the underlying mechanism. Virus inactivation, e.g., through DNA methylation (Brooks et al., 2004), could have accounted for part of the recovery from TeLC-mediated neuronal silencing. However, recovery occurred similarly in ablation experiments, leaving neuronal and synaptic plasticity as the most likely mechanisms. Such compensatory plasticity may involve a downregulation of excitatory input, changes in descending pain control, or the sprouting of inhibitory axons surviving in the ablated area. It is certainly appealing to think that a facilitation of such mechanisms might be exploited therapeutically in chronic pain states.

Control of Itch-Transmitting Circuits by Glycinergic Neurons

The extensive licking and biting behavior and hair loss after glycinergic neuron ablation or silencing together with the suppression of itch responses by activation of local glycinergic neurons indicate that these neurons control not only pain but also itch processing. The intense innervation of glycinergic dorsal horn neurons by myelinated primary sensory neurons fits nicely with the concept of the gate control theory for pain, where light touch has been proposed to reduce transmission of painful signals. However, 9% of the retrogradely labeled primary sensory neurons were peptidergic or bound IB4. These presumed nociceptors likely innervate the small population of glycinergic neurons in the superficial dorsal horn. It is tempting to speculate that these primary sensory fibers and glycinergic neurons underlie the reduction of itch sensations by painful stimulation (Davidson et al., 2009; Ward et al., 1996).

Two previous reports (Kardon et al., 2014; Ross et al., 2010) have identified subpopulations of inhibitory dorsal horn neurons as a source of spinal itch inhibition. These subpopulations depend on the transcription factor Bhlhb5 and express galanin and/or nNOS (Kardon et al., 2014). In the rat, many of the inhibitory nNOS-positive neurons are also glycinergic (Laing et al., 1994), whereas most of the galanin+ neurons are likely purely GABAergic (Simmons et al., 1995). Our studies (Figure S2) indicate that this is also true for the mouse. Therefore, the ablation of the nNOS+ subpopulation of glycinergic neurons may underlie the induction of itch behavior observed in our study. On the other hand, Kardon et al. (2014) provided evidence that the inhibition of itch by dorsal horn interneurons depends on the action of the opioid peptide dynorphin, which is found in the galanin+ subpopulation of purely GABAergic (non-glycinergic) interneurons (Sardella et al., 2011). The latter scenario would suggest the presence of at least two different subsets of dorsal horn inhibitory neurons controlling itch.

Future Implications

This study establishes glycinergic neurons of the dorsal horn as critical elements of a spinal gate for pain and itch signals. It is likely that inhibitory dorsal horn neurons contribute to other spinal cord functions in addition to pain and itch control. Such functions may include improvement of tactile acuity through lateral inhibition (Isaacson and Scanziani, 2011) or of posture and gait control through feedback and feedforward inhibition in motor circuits (Goulding, 2009). It will be interesting to investigate whether these different functions involve distinct glycinergic subpopulations. The virus-based techniques established here constitute a versatile set of tools to address these questions.

EXPERIMENTAL PROCEDURES

Mice

GlyT2::eGFP (Tg(Scl6a5-EGFP)1Uze) and vGAT::ChR2-eYFP (Tg(Slc32a1-COP4*H134R/EYFP)8Gfng) mice have been described previously (Zeilhofer et al., 2005; Zhao et al., 2011). GlyT2::Cre (Tg(Slc6a5-Cre)1Uze) mice were generated following the same strategy as used previously for GlyT2::eGFP mice (Zeilhofer et al., 2005). Control experiments were performed in *Gad67*^{eGFP} (Gad1^{tm1Tama}) mice (Tamamaki et al., 2003) and *ROSA26*^{lacZ} (Gt(ROSA)26Sor) mice (Soriano, 1999). For details, see Supplemental Experimental Procedures. All procedures involving animals were approved by the Veterinäramt des Kantons Zürich (license numbers 64/2010, 75/2010, 75/2013, and 86/2013).

Immunohistochemistry and Image Analysis

Immunohistochemistry was performed as described previously (Punnakkal et al., 2014). For information on antibodies, see Supplemental Experimental Procedures. Fluorescent images were acquired on a Zeiss LSM710 Pascal confocal microscope. For quantitative analyses, sections were prepared from at least three animals, and at least three sections were analyzed per animal. Numbers of immunoreactive cells were determined using the ImageJ Cell Counter plugin. Controlled mean fluorescent intensity (CMTF) was quantified using ImageJ.

Virus Production and Injections

AAV.flex.hM3Dq-mCherry and AVV.eGFP were obtained from the University of North Carolina (UNC) vector core and Penn Vector Core (Perelman School of Medicine, University of Pennsylvania), respectively. All other AAV vectors were cloned in-house and packaged at the Penn Vector Core. The cell lines required for production of EnvA.RabiesΔG-eGFP were obtained from Dr. Edward Callaway (Salk Institute). Propagation was done following the protocol by Osakada and Callaway (2013).

Virus injections were made in mice anesthetized with 2%–5% isoflurane and immobilized on a motorized stereotaxic frame (David Kopf Instruments and Neurostar). Lumbar vertebrae L4 and L5 were exposed, and the vertebral column was fixed using a pair of spinal adaptors. Injections were made at a rate of 30 nl/min with glass micropipettes (tip diameter, 30–40 μm) attached to a 10-μl Hamilton syringe.

Electrophysiology and Optogenetics

Transverse lumbar spinal cord slices were cut from 25- to 28-day-old vGAT::ChR2-eYFP;GlyT2::Cre double-transgenic and vGAT::ChR2-eYFP control (GlyT2::Cre–) mice injected at lumbar levels L3–L5 with a combination of AAV.flex.DTA and AAV.mCherry. Whole-cell patch-clamp recordings were made at room temperature from excitatory superficial dorsal horn neurons. Light-evoked IPSCs were elicited at a frequency of 5min by wide-field illumination of the dorsal horn (473 ± 5 nm wavelength, 2.7 mW, 4 ms).

Behavioral Analyses

Adult male GlyT2::Cre+ and GlyT2::Cre– mice (7–8 weeks old) received three unilateral injections at lumbar levels L3–L5 with AAV.flex.DTA, AAV.flex.TeLC, or AAV.flex.hM3Dq-mCherry. In GlyT2::Cre+ and GlyT2::Cre– mice injected with AAV.flex.DTA and AAV.flex.TeLC, mechanical, heat, and noxious cold sensitivity were assessed for up to 26 days after virus injection. Pharmacogenetic experiments with CNO (1 mg/kg, i.p.) were done in

AAV.flex.hM3Dq-mCherry-injected mice 7 days after CCI surgery (i.e., 14 days after virus injection). Itch responses (flinches and biting bouts) were elicited through intracutaneous injections of chloroquine (10 μl of 8 mg/ml) or histamine (10 μl of 10 mg/ml) into one hindpaw. Animals were videotaped for 30 min, and responses were analyzed offline. The horizontal wire test and the rotarod test were used to assess muscle relaxation and motor impairment, respectively.

SUPPLEMENTAL INFORMATION

Supplemental Information includes Supplemental Experimental Procedures and six figures and can be found with this article online at http://dx.doi.org/10.1016/j.neuron.2015.02.028.

AUTHOR CONTRIBUTIONS

E.F. performed all virus injections and surgeries and performed and analyzed the behavioral experiments except for the pharmacogenetic study. H.W. designed the viral vectors and performed and analyzed the morphological experiments. M.B. performed the pronucleus injections. M.J. and H.W. characterized the GlyT2::Cre mice. H.J. and L.T. performed and analyzed the optogenetic experiments. L.H. contributed to the itch experiments. K.H. established pseudotyped rabies virus production in our group and provided pseudotyped rabies virus for the experiments. W.T.R. and S.H. performed and analyzed the pharmacogenetic experiments. K.K.C. and A.G. provided first stocks of rabies viruses for the retrograde labeling experiments. E.F., H.W., and H.U.Z. designed experiments and wrote the manuscript. All authors commented on the manuscript.

ACKNOWLEDGMENTS

This work was supported by an ERC Advanced Investigator Grant (DHISP 250128) and by grants from the Swiss National Research Foundation (131093 and 156393) (to H.U.Z.) and by the DFG (SFB 870 Neuronal Circuits) (to K.K.C. and A.G.). Dr. Ron Yu (Stowers Institute for Medical Research) provided the plasmid containing the TeLC cds (pGEMT-EZ-TeTx), Dr. Karl Deisseroth (Stanford University) provided the pAAV-Ef1a-DIO-hChR2(H134R)-mCherry-WPRE-pA plasmid, and Dr. Edward M. Callaway (Salk Institute) provided the material required for amplification of G-deficient rabies virus.

Received: September 30, 2014
Revised: January 26, 2015
Accepted: February 12, 2015
Published: March 18, 2015

REFERENCES

Ahmadi, S., Lippross, S., Neuhuber, W.L., and Zeilhofer, H.U. (2002). PGE_2 selectively blocks inhibitory glycinergic neurotransmission onto rat superficial dorsal horn neurons. Nat. Neurosci. *5*, 34–40.

Akiyama, T., and Carstens, E. (2013). Neural processing of itch. Neuroscience *250*, 697–714.

Alexander, G.M., Rogan, S.C., Abbas, A.I., Armbruster, B.N., Pei, Y., Allen, J.A., Nonneman, R.J., Hartmann, J., Moy, S.S., Nicolelis, M.A., et al. (2009). Remote control of neuronal activity in transgenic mice expressing evolved G protein-coupled receptors. Neuron *63*, 27–39.

Armbruster, B.N., Li, X., Pausch, M.H., Herlitze, S., and Roth, B.L. (2007). Evolving the lock to fit the key to create a family of G protein-coupled receptors potently activated by an inert ligand. Proc. Natl. Acad. Sci. USA *104*, 5163–5168.

Aschauer, D.F., Kreuz, S., and Rumpel, S. (2013). Analysis of transduction efficiency, tropism and axonal transport of AAV serotypes 1, 2, 5, 6, 8 and 9 in the mouse brain. PLoS ONE *8*, e76310.

Atasoy, D., Aponte, Y., Su, H.H., and Sternson, S.M. (2008). A FLEX switch targets Channelrhodopsin-2 to multiple cell types for imaging and long-range circuit mapping. J. Neurosci. *28*, 7025–7030.

Baba, H., Ji, R.R., Kohno, T., Moore, K.A., Ataka, T., Wakai, A., Okamoto, M., and Woolf, C.J. (2003). Removal of GABAergic inhibition facilitates polysynaptic A fiber-mediated excitatory transmission to the superficial spinal dorsal horn. Mol. Cell. Neurosci. *24*, 818–830.

Bennett, G.J., and Xie, Y.K. (1988). A peripheral mononeuropathy in rat that produces disorders of pain sensation like those seen in man. Pain *33*, 87–107.

Betley, J.N., and Sternson, S.M. (2011). Adeno-associated viral vectors for mapping, monitoring, and manipulating neural circuits. Hum. Gene Ther. *22*, 669–677.

Beyer, C., Roberts, L.A., and Komisaruk, B.R. (1985). Hyperalgesia induced by altered glycinergic activity at the spinal cord. Life Sci. *37*, 875–882.

Bráz, J.M., Sharif-Naeini, R., Vogt, D., Kriegstein, A., Alvarez-Buylla, A., Rubenstein, J.L., and Basbaum, A.I. (2012). Forebrain GABAergic neuron precursors integrate into adult spinal cord and reduce injury-induced neuropathic pain. Neuron *74*, 663–675.

Brooks, A.R., Harkins, R.N., Wang, P., Qian, H.S., Liu, P., and Rubanyi, G.M. (2004). Transcriptional silencing is associated with extensive methylation of the CMV promoter following adenoviral gene delivery to muscle. J. Gene Med. *6*, 395–404.

Buch, T., Heppner, F.L., Tertilt, C., Heinen, T.J., Kremer, M., Wunderlich, F.T., Jung, S., and Waisman, A. (2005). A Cre-inducible diphtheria toxin receptor mediates cell lineage ablation after toxin administration. Nat. Methods *2*, 419–426.

Chamberlin, N.L., Du, B., de Lacalle, S., and Saper, C.B. (1998). Recombinant adeno-associated virus vector: use for transgene expression and anterograde tract tracing in the CNS. Brain Res. *793*, 169–175.

Clark, A.K., Gentry, C., Bradbury, E.J., McMahon, S.B., and Malcangio, M. (2007). Role of spinal microglia in rat models of peripheral nerve injury and inflammation. Eur. J. Pain *11*, 223–230.

Coull, J.A., Boudreau, D., Bachand, K., Prescott, S.A., Nault, F., Sík, A., De Koninck, P., and De Koninck, Y. (2003). Trans-synaptic shift in anion gradient in spinal lamina I neurons as a mechanism of neuropathic pain. Nature *424*, 938–942.

Coull, J.A., Beggs, S., Boudreau, D., Boivin, D., Tsuda, M., Inoue, K., Gravel, C., Salter, M.W., and De Koninck, Y. (2005). BDNF from microglia causes the shift in neuronal anion gradient underlying neuropathic pain. Nature *438*, 1017–1021.

Coyle, D.E. (1998). Partial peripheral nerve injury leads to activation of astroglia and microglia which parallels the development of allodynic behavior. Glia *23*, 75–83.

Davidson, S., Zhang, X., Khasabov, S.G., Simone, D.A., and Giesler, G.J., Jr. (2009). Relief of itch by scratching: state-dependent inhibition of primate spinothalamic tract neurons. Nat. Neurosci. *12*, 544–546.

Drew, G.M., Siddall, P.J., and Duggan, A.W. (2004). Mechanical allodynia following contusion injury of the rat spinal cord is associated with loss of GABAergic inhibition in the dorsal horn. Pain *109*, 379–388.

Duan, B., Cheng, L., Bourane, S., Britz, O., Padilla, C., Garcia-Campmany, L., Krashes, M., Knowlton, W., Velasquez, T., Ren, X., et al. (2014). Identification of spinal circuits transmitting and gating mechanical pain. Cell *159*, 1417–1432.

Gomeza, J., Ohno, K., Hülsmann, S., Armsen, W., Eulenburg, V., Richter, D.W., Laube, B., and Betz, H. (2003). Deletion of the mouse glycine transporter 2 results in a hyperekplexia phenotype and postnatal lethality. Neuron *40*, 797–806.

Goulding, M. (2009). Circuits controlling vertebrate locomotion: moving in a new direction. Nat. Rev. Neurosci. *10*, 507–518.

Graeber, M.B., and Christie, M.J. (2012). Multiple mechanisms of microglia: a gatekeeper's contribution to pain states. Exp. Neurol. *234*, 255–261.

Hanisch, U.K., and Kettenmann, H. (2007). Microglia: active sensor and versatile effector cells in the normal and pathologic brain. Nat. Neurosci. *10*, 1387–1394.

Harvey, R.J., Depner, U.B., Wässle, H., Ahmadi, S., Heindl, C., Reinold, H., Smart, T.G., Harvey, K., Schütz, B., Abo-Salem, O.M., et al. (2004). GlyR α3: an essential target for spinal PGE_2-mediated inflammatory pain sensitization. Science *304*, 884–887.

Hossaini, M., French, P.J., and Holstege, J.C. (2007). Distribution of glycinergic neuronal somata in the rat spinal cord. Brain Res. *1142*, 61–69.

Hutson, T.H., Verhaagen, J., Yáñez-Muñoz, R.J., and Moon, L.D. (2012). Corticospinal tract transduction: a comparison of seven adeno-associated viral vector serotypes and a non-integrating lentiviral vector. Gene Ther. *19*, 49–60.

Isaacson, J.S., and Scanziani, M. (2011). How inhibition shapes cortical activity. Neuron *72*, 231–243.

Kardon, A.P., Polgár, E., Hachisuka, J., Snyder, L.M., Cameron, D., Savage, S., Cai, X., Karnup, S., Fan, C.R., Hemenway, G.M., et al. (2014). Dynorphin acts as a neuromodulator to inhibit itch in the dorsal horn of the spinal cord. Neuron *82*, 573–586.

Keller, A.F., Coull, J.A., Chery, N., Poisbeau, P., and De Koninck, Y. (2001). Region-specific developmental specialization of GABA-glycine cosynapses in laminas I-II of the rat spinal dorsal horn. J. Neurosci. *21*, 7871–7880.

Keller, A.F., Beggs, S., Salter, M.W., and De Koninck, Y. (2007). Transformation of the output of spinal lamina I neurons after nerve injury and microglia stimulation underlying neuropathic pain. Mol. Pain *3*, 27.

Knabl, J., Witschi, R., Hösl, K., Reinold, H., Zeilhofer, U.B., Ahmadi, S., Brockhaus, J., Sergejeva, M., Hess, A., Brune, K., et al. (2008). Reversal of pathological pain through specific spinal $GABA_A$ receptor subtypes. Nature *451*, 330–334.

Kuner, R. (2010). Central mechanisms of pathological pain. Nat. Med. *16*, 1258–1266.

Laing, I., Todd, A.J., Heizmann, C.W., and Schmidt, H.H. (1994). Subpopulations of GABAergic neurons in laminae I-III of rat spinal dorsal horn defined by coexistence with classical transmitters, peptides, nitric oxide synthase or parvalbumin. Neuroscience *61*, 123–132.

Loomis, C.W., Khandwala, H., Osmond, G., and Hefferan, M.P. (2001). Coadministration of intrathecal strychnine and bicuculline effects synergistic allodynia in the rat: an isobolographic analysis. J. Pharmacol. Exp. Ther. *296*, 756–761.

Lu, Y., Dong, H., Gao, Y., Gong, Y., Ren, Y., Gu, N., Zhou, S., Xia, N., Sun, Y.Y., Ji, R.R., and Xiong, L. (2013). A feed-forward spinal cord glycinergic neural circuit gates mechanical allodynia. J. Clin. Invest. *123*, 4050–4062.

Melzack, R., and Wall, P.D. (1965). Pain mechanisms: a new theory. Science *150*, 971–979.

Miraucourt, L.S., Moisset, X., Dallel, R., and Voisin, D.L. (2009). Glycine inhibitory dysfunction induces a selectively dynamic, morphine-resistant, and neurokinin 1 receptor- independent mechanical allodynia. J. Neurosci. *29*, 2519–2527.

Moore, K.A., Kohno, T., Karchewski, L.A., Scholz, J., Baba, H., and Woolf, C.J. (2002). Partial peripheral nerve injury promotes a selective loss of GABAergic inhibition in the superficial dorsal horn of the spinal cord. J. Neurosci. *22*, 6724–6731.

Müller, F., Heinke, B., and Sandkühler, J. (2003). Reduction of glycine receptor-mediated miniature inhibitory postsynaptic currents in rat spinal lamina I neurons after peripheral inflammation. Neuroscience *122*, 799–805.

Osakada, F., and Callaway, E.M. (2013). Design and generation of recombinant rabies virus vectors. Nat. Protoc. *8*, 1583–1601.

Palmiter, R.D., Behringer, R.R., Quaife, C.J., Maxwell, F., Maxwell, I.H., and Brinster, R.L. (1987). Cell lineage ablation in transgenic mice by cell-specific expression of a toxin gene. Cell *50*, 435–443.

Polgár, E., Durrieux, C., Hughes, D.I., and Todd, A.J. (2013). A quantitative study of inhibitory interneurons in laminae I-III of the mouse spinal dorsal horn. PLoS ONE *8*, e78309.

Poyatos, I., Ponce, J., Aragón, C., Giménez, C., and Zafra, F. (1997). The glycine transporter GLYT2 is a reliable marker for glycine-immunoreactive neurons. Brain Res. Mol. Brain Res. *49*, 63–70.

Punnakkal, P., von Schoultz, C., Haenraets, K., Wildner, H., and Zeilhofer, H.U. (2014). Morphological, biophysical and synaptic properties of glutamatergic neurons of the mouse spinal dorsal horn. J. Physiol. *592*, 759–776.

Ross, S.E., Mardinly, A.R., McCord, A.E., Zurawski, J., Cohen, S., Jung, C., Hu, L., Mok, S.I., Shah, A., Savner, E.M., et al. (2010). Loss of inhibitory interneurons in the dorsal spinal cord and elevated itch in *Bhlhb5* mutant mice. Neuron *65*, 886–898.

Sandkühler, J. (2009). Models and mechanisms of hyperalgesia and allodynia. Physiol. Rev. *89*, 707–758.

Sardella, T.C., Polgár, E., Garzillo, F., Furuta, T., Kaneko, T., Watanabe, M., and Todd, A.J. (2011). Dynorphin is expressed primarily by GABAergic neurons that contain galanin in the rat dorsal horn. Mol. Pain *7*, 76.

Scholz, J., Broom, D.C., Youn, D.H., Mills, C.D., Kohno, T., Suter, M.R., Moore, K.A., Decosterd, I., Coggeshall, R.E., and Woolf, C.J. (2005). Blocking caspase activity prevents transsynaptic neuronal apoptosis and the loss of inhibition in lamina II of the dorsal horn after peripheral nerve injury. J. Neurosci. *25*, 7317–7323.

Sherman, S.E., and Loomis, C.W. (1994). Morphine insensitive allodynia is produced by intrathecal strychnine in the lightly anesthetized rat. Pain *56*, 17–29.

Simmons, D.R., Spike, R.C., and Todd, A.J. (1995). Galanin is contained in GABAergic neurons in the rat spinal dorsal horn. Neurosci. Lett. *187*, 119–122.

Sivilotti, L., and Woolf, C.J. (1994). The contribution of $GABA_A$ and glycine receptors to central sensitization: disinhibition and touch-evoked allodynia in the spinal cord. J. Neurophysiol. *72*, 169–179.

Soriano, P. (1999). Generalized lacZ expression with the ROSA26 Cre reporter strain. Nat. Genet. *21*, 70–71.

Sorkin, L.S., Puig, S., and Jones, D.L. (1998). Spinal bicuculline produces hypersensitivity of dorsal horn neurons: effects of excitatory amino acid antagonists. Pain *77*, 181–190.

Sweeney, S.T., Broadie, K., Keane, J., Niemann, H., and O'Kane, C.J. (1995). Targeted expression of tetanus toxin light chain in Drosophila specifically eliminates synaptic transmission and causes behavioral defects. Neuron *14*, 341–351.

Tamamaki, N., Yanagawa, Y., Tomioka, R., Miyazaki, J., Obata, K., and Kaneko, T. (2003). Green fluorescent protein expression and colocalization with calretinin, parvalbumin, and somatostatin in the GAD67-GFP knock-in mouse. J. Comp. Neurol. *467*, 60–79.

Tanga, F.Y., Raghavendra, V., and DeLeo, J.A. (2004). Quantitative real-time RT-PCR assessment of spinal microglial and astrocytic activation markers in a rat model of neuropathic pain. Neurochem. Int. *45*, 397–407.

Taves, S., Berta, T., Chen, G., and Ji, R.R. (2013). Microglia and spinal cord synaptic plasticity in persistent pain. Neural Plast. *2013*, 753656.

Todd, A.J., and Spike, R.C. (1993). The localization of classical transmitters and neuropeptides within neurons in laminae I-III of the mammalian spinal dorsal horn. Prog. Neurobiol. *41*, 609–645.

Torsney, C., and MacDermott, A.B. (2006). Disinhibition opens the gate to pathological pain signaling in superficial neurokinin 1 receptor-expressing neurons in rat spinal cord. J. Neurosci. *26*, 1833–1843.

Ward, L., Wright, E., and McMahon, S.B. (1996). A comparison of the effects of noxious and innocuous counterstimuli on experimentally induced itch and pain. Pain *64*, 129–138.

Wickersham, I.R., Lyon, D.C., Barnard, R.J., Mori, T., Finke, S., Conzelmann, K.K., Young, J.A., and Callaway, E.M. (2007). Monosynaptic restriction of transsynaptic tracing from single, genetically targeted neurons. Neuron *53*, 639–647.

Woolf, C.J., and Salter, M.W. (2000). Neuronal plasticity: increasing the gain in pain. Science *288*, 1765–1769.

Xiong, W., Cheng, K., Cui, T., Godlewski, G., Rice, K.C., Xu, Y., and Zhang, L. (2011). Cannabinoid potentiation of glycine receptors contributes to cannabis-induced analgesia. Nat. Chem. Biol. *7*, 296–303.

Xiong, W., Cui, T., Cheng, K., Yang, F., Chen, S.R., Willenbring, D., Guan, Y., Pan, H.L., Ren, K., Xu, Y., and Zhang, L. (2012). Cannabinoids suppress inflammatory and neuropathic pain by targeting α3 glycine receptors. J. Exp. Med. *209*, 1121–1134.

Yaksh, T.L. (1989). Behavioral and autonomic correlates of the tactile evoked allodynia produced by spinal glycine inhibition: effects of modulatory receptor systems and excitatory amino acid antagonists. Pain *37*, 111–123.

Zeilhofer, H.U., Studler, B., Arabadzisz, D., Schweizer, C., Ahmadi, S., Layh, B., Bösl, M.R., and Fritschy, J.M. (2005). Glycinergic neurons expressing enhanced green fluorescent protein in bacterial artificial chromosome transgenic mice. J. Comp. Neurol. *482*, 123–141.

Zeilhofer, H.U., Wildner, H., and Yévenes, G.E. (2012). Fast synaptic inhibition in spinal sensory processing and pain control. Physiol. Rev. *92*, 193–235.

Zhao, S., Ting, J.T., Atallah, H.E., Qiu, L., Tan, J., Gloss, B., Augustine, G.J., Deisseroth, K., Luo, M., Graybiel, A.M., and Feng, G. (2011). Cell type–specific channelrhodopsin-2 transgenic mice for optogenetic dissection of neural circuitry function. Nat. Methods *8*, 745–752.

Neuron

Supplemental Information

Targeted Ablation, Silencing, and Activation Establish Glycinergic Dorsal Horn Neurons as Key Components of a Spinal Gate for Pain and Itch

Edmund Foster, Hendrik Wildner, Laetitia Tudeau, Sabine Haueter, William T. Ralvenius, Monika Jegen, Helge Johannssen, Ladina Hösli, Karen Haenraets, Alexander Ghanem, Karl-Klaus Conzelmann, Michael Bösl, Hanns Ulrich Zeilhofer

Supplemental Data

Supplemental Figures

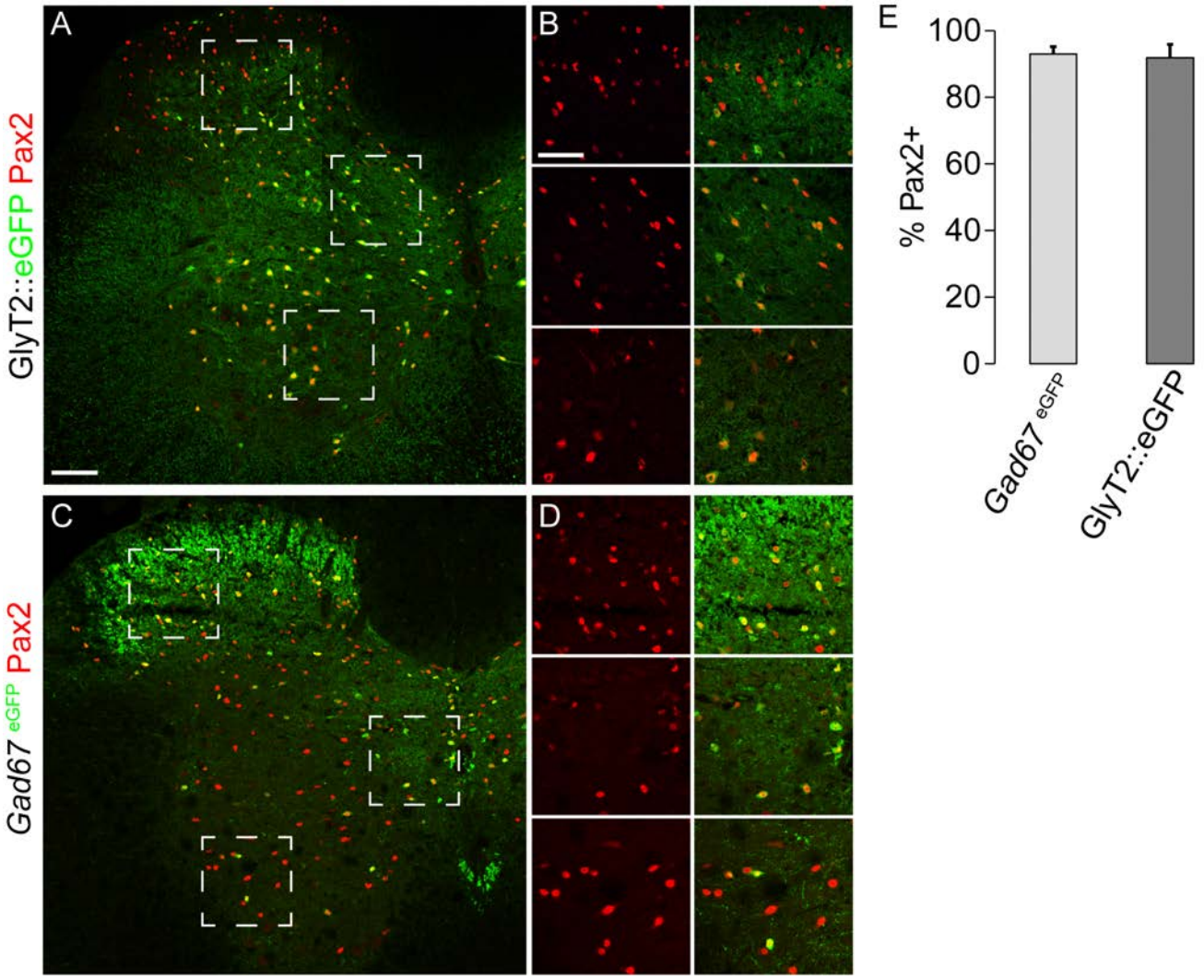

Figure S1 (related to Figure 1). Pax2 expression is maintained in inhibitory interneurons of the mouse spinal cord into adulthood

(A - D) At P60, Pax2 (red) expression is detectable in nearly all eGFP+ cells of GlyT2::eGFP and *Gad67*^{eGFP} transgenic mice. Magnifications in B and D correspond to the indicated areas in A and C, respectively. (E) Quantification of the number of eGFP+ neurons in *Gad67*^{eGFP} and GlyT2::eGFP transgenic mice also expressing Pax2. Mean ± SD. Scale bars: (A) 100 µm (B) 50 µm.

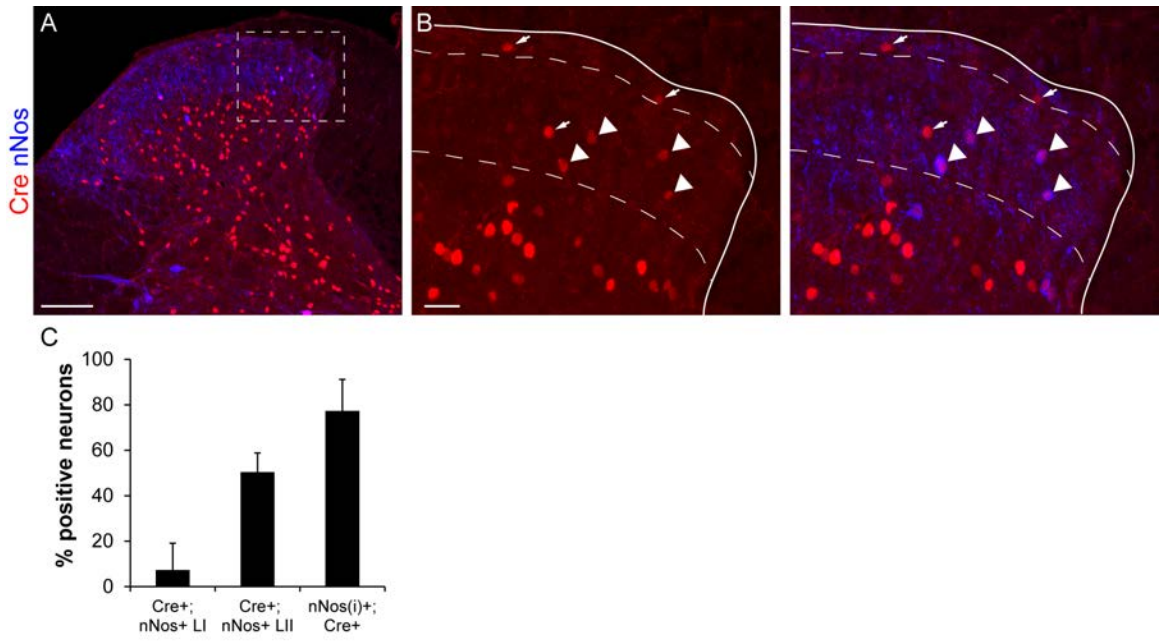

Figure S2 (related to Figure 1). nNos coexpression in superficial dorsal horn GlyT2::Cre+ neurons. (A) Spinal dorsal horn section of a GlyT2::Cre transgenic mouse stained against Cre and nNos proteins. Sections were co-stained for Pax2 to restrict analyses to inhibitory dorsal horn neuron. (B) Higher magnification. Arrowheads indicate double labeled neurons. Arrows indicate Cre+ / nNos- neurons. (C) Percentage of Cre+ neurons expressing nNos in laminae I (Cre+;nNos+ LI) and laminae II (Cre+;nNos+ LII) were determined as well as the percentage of inhibitory nNos neurons expressing Cre (nNos(i)+; Cre). To restrict the quantitative analysis to inhibitory nNos (nNos(i)+) dorsal horn neurons sections were co-stained for Pax2. Mean ± SD (n = 9 section from 3 mice). Scale bars, (A) 100 µm (B) 20 µm.

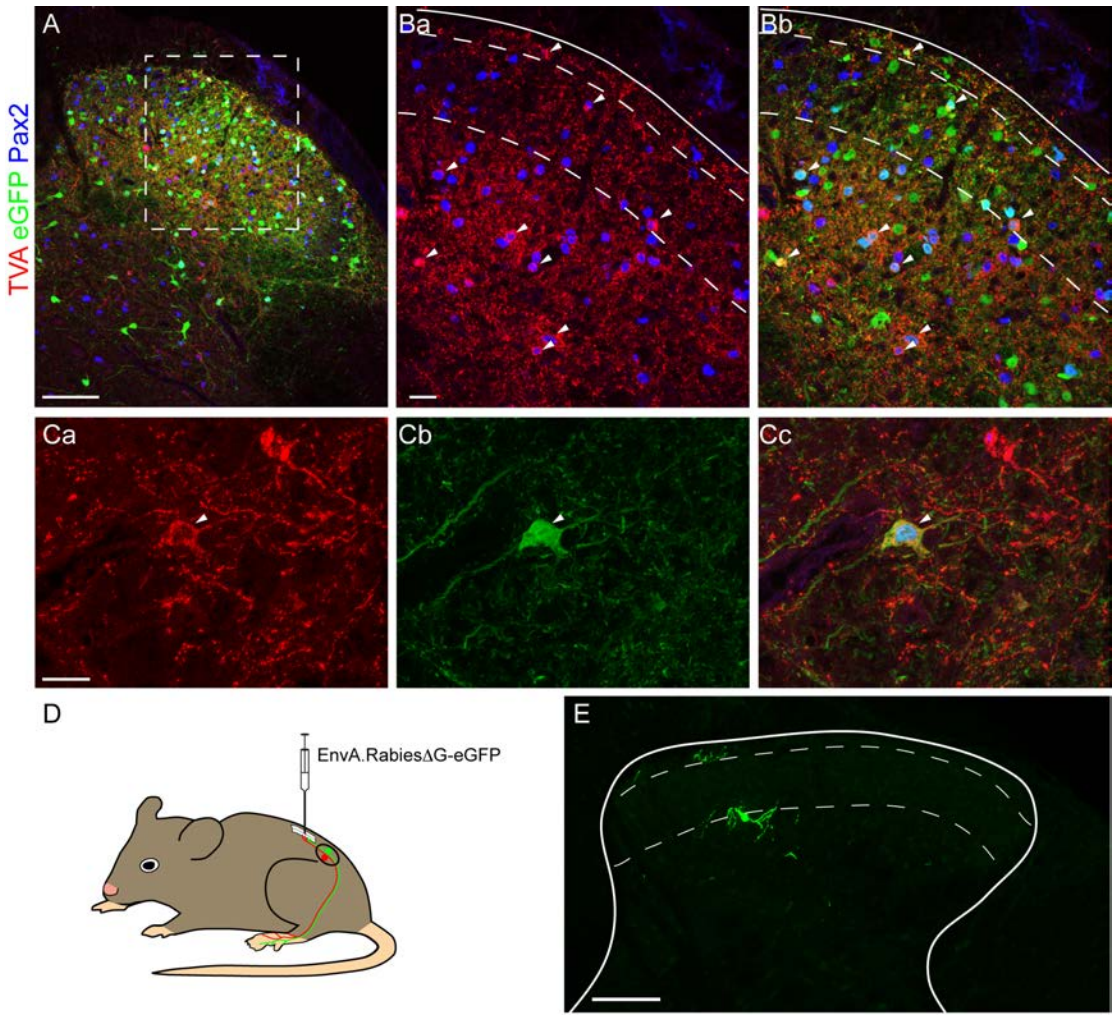

Figure S3 (related to Figure 2). Rabies virus-infected neurons 7 days after rabies virus injection into the spinal dorsal horn. (A - C) Spinal cord of GlyT2::Cre mice injected first with AAV.flex.TVA-2A-RabG and then with EnvA.RabiesΔG-eGFP. (A) Representative section of an injected spinal cord labeled with antibodies against TVA (red), eGFP (green) and Pax2 (blue). (Ba,b) Higher resolution picture demonstrating the presence of multiple primary infected cells (arrowheads, triple labeled cells). (Ca-c) Example of a neuron expressing TVA, GFP and Pax2. On average, 30 - 40 triple labeled cells were identified per section. From serial sections, we estimate that primary EnvA.RabiesΔG-eGFP infection occurred in about 2500 cells / spinal cord (n = 8 mice). (D, E) When EnvA.RabiesΔG-eGFP was injected into non-preinfected (TVA-negative) GlyT2::Cre mice, eGFP+ neurons occurred occasionally (0 - 7 cells / spinal cord, n = 4 mice), most likely due to very small contaminations of the EnvA.RabiesΔG-eGFP virus stock with non-pseudotyped virus. Scale bars, 100 µm (A, E), 20 µm (B, C).

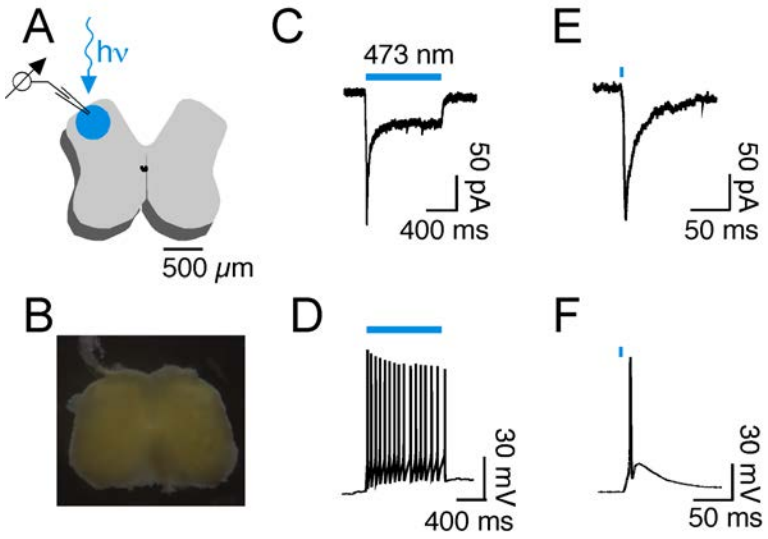

Figure S4 (related to Figure 4) Optogenetic characterization of inhibitory dorsal horn neurons. (A) Photocurrents and light-evoked action potentials in neurons recorded from slices obtained from vGAT::ChR2-eYFP BAC transgenic mice. (A) Blue light of 473 ± 5 nm wavelength was applied to one entire dorsal horn. (B) Distribution of the ChR2-eYFP fluorescence in a horizontal lumbar spinal cord slice. (C) Partially desensitizing photocurrent recorded from a lamina II neuron evoked by 1 s light exposure. (D) The same light stimulus evoked a train of action potentials in the current clamp mode, which is typical of inhibitory neurons in the superficial mouse spinal dorsal horn (Punnakkal et al., 2014). (E) Short photocurrent evoked by a 4 ms light stimulation. (F) Single action potential evoked by a 4 ms light stimulus.

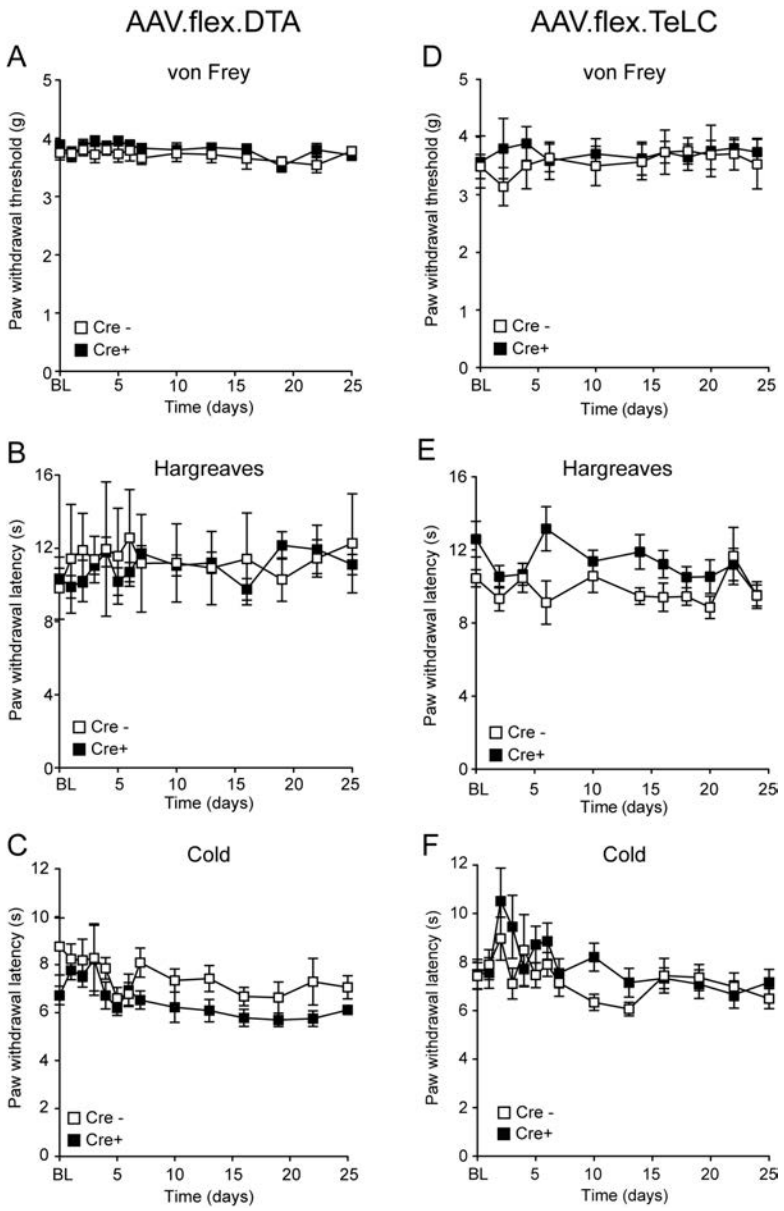

Figure S5 (related to Figures 5 and 7). Contralateral mechanical and thermal responses following contralateral ablation or silencing of spinal glycinergic neurons.

(A - C) Mechanical (A), heat (B), and noxious cold (C) sensitivities for the contralateral paw remained virtually unchanged after AAV.flex.DTA injection. Repeated measures ANOVA did not reveal significant genotype x time interactions between GlyT2::Cre+ and GlyT2::Cre- mice (von Frey: $F(13,221) = 0.57$, $P = 0.87$; Hargreaves: $F(13,221) = 1.06$, $P = 0.39$; cold: $F(13,143) = 0.44$, $P = 0.96$). (D - F) No mechanical and thermal sensitization developed after AAV.flex.TeLC injection. Repeated measures ANOVA: von Frey: $F(10,140) = 1.12$, $P = 0.35$; Hargreaves: $F(10,140) = 1.38$, $P = 0.20$; cold: $F(13,247) = 0.97$, $P = 0.48$). All error bars are SEM.

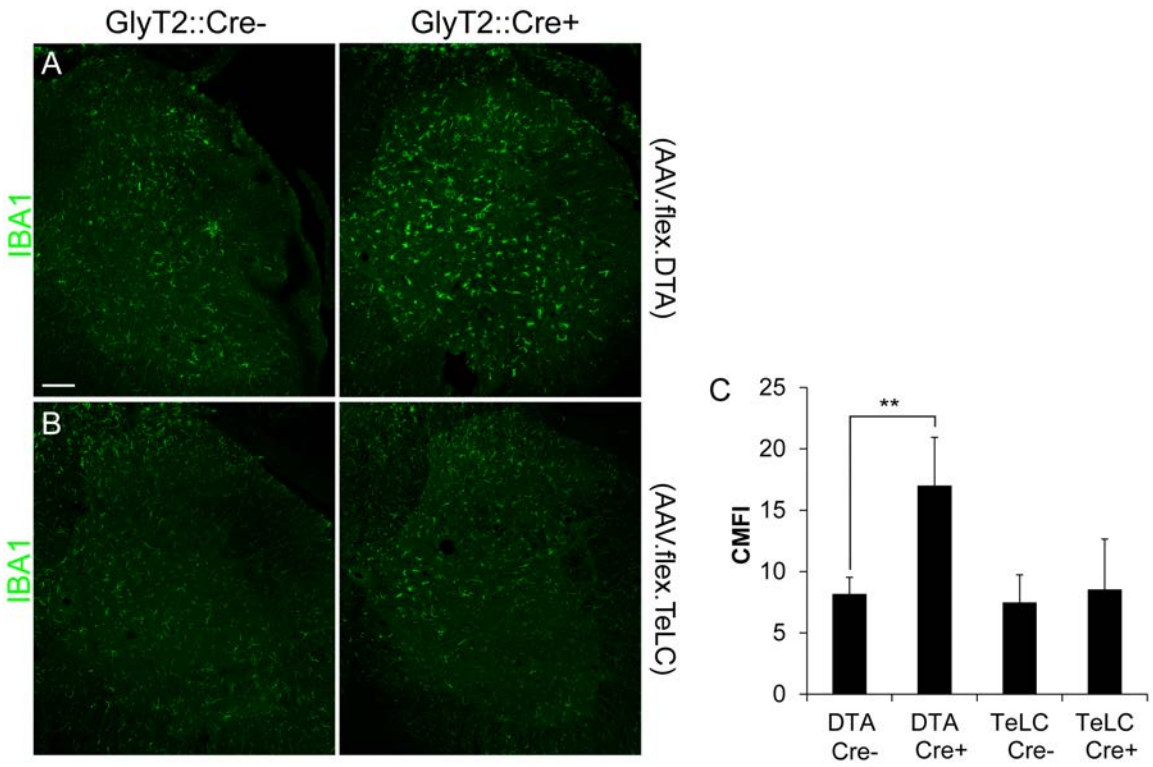

Figure S6 (related to Figure 6). Microglia activation after intraspinal AAV injection

Sections of spinal cords injected with either AAV.flex.DTA (A) or AAV.flex.TeLC (B) were stained with anti-IBA1 (green) antibodies to assess microglia activation. (A) An increased IBA1 immunoreactivity was observed 4 d after AAV.flex.DTA injection into the dorsal horn of GlyT2::Cre+ (Cre) mice compared to GlyT2::Cre- littermates. (B) After AAV.flex.TeLC injection no obvious difference in IBA1 intensity was observed when comparing spinal cord sections from Cre+ or Cre- mice. (C) Quantification of the corrected mean fluorescence intensity (CMFI, mean ± SD) in spinal cord sections after the injection of AAV.flex.DTA (DTA) or AAV.flex.TeLC (TeLC) into GlyT2::Cre+ or GlyT2::Cre- mice. Statistics: **, $P < 0.01$ (unpaired t-test), data are from 4 – 5 mice of both genotypes, and 3 sections per mouse. Scale bar 100 µm.

Supplemental Experimental Procedures

Generation of GlyT2::Cre mice

Cre cDNA followed by the bovine growth hormone polyadenylation (poly-A) signal was placed in frame into the start of exon 2 of the *GlyT2* (*slc6a5*) gene (on BAC clone RP23-365E4) using homologous recombination in bacteria (Copeland et al., 2001) thereby replacing exon 2 of the *GlyT2* gene. Mice derived from BAC DNA-injected C57BL/6 oocytes were screened by PCR for the presence of Cre and for the two BAC ends. Transgenic mice were maintained on a C57BL/6J background.

Immunohistochemistry

Mice were perfused with 4% paraformaldehyde (PFA) in PBS followed by postfixation in 4% PFA in PBS for 1 - 2 hours. The tissue was cut into 25 µm cryosections, which were mounted onto Superfrost Plus microscope slides (Thermo Scientific, Zurich, Switzerland). The following antibodies were used: goat anti-βGal (1:1000, Abcam, Cambridge, UK), goat anti-CGRP (1:500, Abcam, Cambridge, UK), mouse anti-Cre (1:1000, Abcam, Cambridge, UK), rabbit anti-c-fos (1:5000, Millipore, Billerica MA, USA), rabbit anti-GFP (1:1000 or 1:3000; Molecular Probes Inc., Eugene, OR, USA), sheep anti-eGFP (1:1000; AbD Serotec, Kidlington, UK), rabbit anti-IBA1 (1:1000, Wako, Neuss, Germany), rabbit and guinea pig anti-Lmx1b (1:10,000; gift from Dr Carmen Birchmeier, MDC Berlin), Rabbit anti-NF200 (1:2000, Sigma, St. Louis, US), Rabbit anti-NeuN (1:3000, Abcam, Cambridge, UK), goat anti-nNos (1:1000, Abcam, Cambridge, UK), goat anti-Pax2 (1:200, R&D systems, Minneapolis, US), rabbit anti-Pax2 (1:400; Invitrogen, Carlsbad, USA), rabbit anti-PKCγ (1:1000; Santa Cruz, Dallas, TX, USA), rabbit anti-TVA (generous gift from D. Saur; Seidler et al., 2008), rabbit anti-vAChT (1 : 2000; Synaptic Systems, Göttingen, Germany) and cyanine 3 (Cy3)-, Alexa Fluor 488-, DyLight 488-, 647- and 649-conjugated donkey secondary antibodies (Dianova, Hamburg, Germany). To detect IB4+ neurons the isolectin IB4 Alexa Fluor 647 conjugate (Life Technologies, Carlsbad, US) was used.

Image analysis

Fluorescent images were acquired on a Zeiss LSM710 Pascal confocal microscope using a 0.8 NA × 20 Plan-apochromat objective or a 1.3 NA × 40 EC Plan-Neofluar oil-immersion objective and the ZEN2012 software (Carl Zeiss). Whenever applicable, contrast, illumination, and false colors were adjusted in ImageJ or Adobe Photoshop (Adobe Systems, Dublin, Ireland). For cell counts in tissue sections, section were prepared from at least three animals and at least three sections were analyzed per animal. In order to avoid double counting of cells in adjacent sections, all sections used for quantification were taken at a rostro-caudal distance of at least 50 µm. Numbers of immunoreactive cells were determined using the ImageJ Cell Counter plug-in. In order to quantify controlled mean fluorescent intensity (CMTF) in tissue sections the gray matter in a spinal cord section was selected and the measure function of ImageJ was used to determine the mean fluorescent intensity. The CMTF was calculated by subtracting the mean value of four randomly selected background regions from the mean fluorescent value of the grey matter.

AAV preparation

AAV.flex.DTA and AAV.flex.TeLC vectors were cloned in-house and packaged at Penn Vector Core (Perelman School of Medicine, University of Pennsylvania) using their custom service. AAV.flex.DTA and AAV.flex.TeLC vectors were cloned by excising the ChR2-mCherry fusion protein from pAAV-Ef1a-DIO-hChR2(H134R)-mCherry-WPRE-pA (kindly provided by Dr. Karl Deisseroth, Stanford University) with AscI and NheI and replacing it with PCR amplified DTA or TeLC cDNA. DTA cds was amplified from pDTA vector and TeLC cds was amplified from pGEM-EZ-TeTx plasmid (kind gift of Dr Ron Yu, Stowers Institute for Medical Research, Kansas City, MO). AAV 2/1 vectors were used for all experiments described in this study with the exception of AAV.flex.hM3Dq-mCherry, which was serotype 2 (UNC Vector Core, Chapel Hill, NC) and the eGFP expressing reporter vector, which was serotype 9. All three AAVs have previously been shown to efficiently transduce neurons in the CNS (Weinberg et al., 2013).

Intraspinal AVV injections

Animals were anesthetized with 2 - 5% isofluorane and lumbar vertebrae L4 and L5 were exposed. The animal was then placed in a motorized stereotaxic frame and the vertebral column was immobilized

using a pair of spinal adaptors. The vertebral lamina and dorsal spinous process were removed to expose the L4 lumbar segment. The dura was perforated about 500 µm left of the dorsal blood vessel using a beveled 27G needle. Viral vectors were injected at a depth of 200 - 300 µm using a glass micropipette (tip diameter 30 - 40 µm) attached to a 10 µl Hamilton syringe. The rate of injection (30 nl/min) was controlled using a PHD Ultra syringe pump with a nanomite attachment (Harvard Apparatus, Holliston, MA). The micropipette was left in place for 5 min after the injection. Wounds were sutured and the animals were injected i.p. with 0.03 mg/kg buprenorphine and allowed to recover on a heat mat.

Retrograde tracing experiments

For retrograde monosynaptic tracing experiments, we used a two-step strategy that involved injection an AAV helper virus (AAV.flex.TVA.2A.RbG) containing a Cre-dependent TVA (avian tumor virus receptor A) and rabies glycoprotein (RbG) expression cassette and a subsequent injection of an EnvA (avian sarcoma leukosis virus "A" envelop glycoprotein) pseudotyped glycoprotein-deficient rabies virus (EnvA.RabiesΔG.eGFP). The TVA protein expressed from the helper virus enabled cell type-specific infection of GlyT2::Cre+ neurons, and the RbG was expressed to transcomplement the glycoprotein-deficient rabies virus in the primary infected neurons. GlyT2::Cre+ mice received two unilateral injections of AAV.flex.TVA.2A.RbG (2.9 x 10^9 GC per injection in 300 nl) into L3 and L4 segments of the dorsal horn. The vertebral lamina was left intact in order to limit the adhesion of scar tissue to the dorsal surface of the spinal cord. The mice were allowed to recover and then 14 days before they received an injection of EnvA.RabiesΔG.eGFP (1 x 10^6 GC per injection in 500 nl) into the same site. The brain, spinal cord and DRGs were harvested 7 days later.

Electrophysiology and optogenetics

Optogenetic experiments were made in vGAT::ChR2-eYFP;GlyT2::Cre double transgenic mice and in vGAT::ChR2-eYFP control (GlyT2::Cre-) mice of either sex. At P18, mice received two unilateral injections of AAV.flex.DTA together with AAV.mCherry (both 1 x 10^9 vector particles/ injection). Four to 8 days later, mice were decapitated in deep isoflurane anesthesia. Transverse spinal cord slices were prepared as described by (Dugue et al., 2009). During recordings, slices were continuously superfused with aCSF containing (in mM): 120 NaCl, 2.5 KCl, 1.25 NaH_2PO_4, 26 $NaHCO_3$, 5 HEPES, 1 $MgCl_2$, 2 $CaCl_2$ and 14.6 glucose, equilibrated with 95% O_2, 5% CO_2. Whole-cell patch-clamp recordings were made at room temperature from lamina I/II neurons of the infected area, which could easily be identified by its red fluorescence. Recorded neurons were held at -70 mV using an EPC 9 amplifier (HEKA Elektronik, Lambrecht, Germany) controlled with Patchmaster acquisition software. Patch pipettes (resistance 4 - 5 MΩ) were filled with intracellular solution containing (in mM): 120 CsCl, 2 $MgCl_2$ 6 H_2O, 10 HEPES, 0.05 EGTA, 2 MgATP, 0.1 NaGTP, 5 QX-314 (pH 7.35). Light-evoked IPSCs were elicited at a frequency of 5 / min by wide field illumination of the ispilateral dorsal horn (473 ± 5 nm wave length, 2.7 mW, 4 ms) using a Polychrome V monochromator (Till Photonics, Gräfelfing, Germany). Access resistance was monitored with short hyperpolarizing voltage steps (-5 mV) between the synaptic stimulations.

Behavioral analyses

Adult male GlyT2::Cre+ mice (4 – 5 weeks-old) received three unilaterally injections (300 nl) at level L3 – L5 with AAV.flex.DTA (1 x 10^9 virus particles/injection), AAV.flex.TeLC-FLAG (2 x 10^8 virus particles/injection) or AAV.flex.hM3Dq-mCherry (5 x 10^8 particles/injection). Animals injected with AAV.flex.DTA were also co-injected with AAV.eGFP (1 x 10^9 virus particles/injection). Experimenters were blinded to either genotype or treatment, and only mice that did not show obvious (motor) impairments were used.

Mechanical withdrawal thresholds and thermal withdrawal latencies were assessed using an electronic von Frey anesthesiometer and Hargreaves test apparatus with a temperature controlled glass platform (30°C) (both from IITC, Woodland Hills, CA). Responses to noxious cold were determined following the protocol by (Brenner et al., 2012) using a 5 mm thick borosilicate glass platform. Baseline measurements were recorded on two consecutive days prior to surgery. Six measurements were recorded for each animal, and the ipsilateral and contralateral paws were tested alternately. Motor coordination was tested using an accelerating rotarod (IITC,

Woodland Hills, CA). Mice were trained on 2 consecutive days and the maximum number of rotations per minute (rpm) that caused the animal to fall was recorded. The rod was programmed to accelerate from 0 to 40 rpm over 300 s. On experimental days, each mouse was allowed three trials and the average rpm at the point of failure was recorded. Animals were videotaped for 5 min to allow off-line quantification of spontaneous aversive behaviors (flinching and the time spent licking/biting).

Animals injected with AAV.flex.hM3Dq-mCherry (Alexander et al., 2009) were subjected to a chronic constriction injury of the sciatic nerve (Bennett and Xie, 1988) 7 days post virus injection. Baseline mechanical thresholds were recorded before and after surgery. Seven days post surgery, the animals were injected i.p. with 1 mg/kg clozapine *N*-oxide (CNO, Sigma) or vehicle (saline with 0.5% DMSO) and mechanical sensitivity of the ipsilateral and contralateral paws was measured every 15 min for 5 hours, and 24 hours after drug administration.

The horizontal wire test (Bonetti et al., 1982) was used to assess potential muscle relaxation. Mice were placed forepaws-first onto a metal wire and scored according to whether or not they were able to grasp the wire with their hindpaws.

Itch responses were assessed 14 days after intraspinal AAV.flex.hM3Dq-mCherry injection. Mice were treated with either CNO (1 mg/kg, i.p.) or vehicle. The animals were allowed to settle for 60 min before histamine or chloroquine were intracutaneously injected at the plantar surface of the left hind paw (i.e. ipsilateral to the virus injection).

Statistical analyses

Unless otherwise indicated, all data are given as mean ± SEM. Statistical comparisons were made using unpaired or paired t-tests, one-way ANOVA, repeated measures ANOVA, two-way ANOVA or two-way repeated measures ANOVA followed by appropriate *post hoc* tests.

Supplemental References

Alexander, G.M., Rogan, S.C., Abbas, A.I., Armbruster, B.N., Pei, Y., Allen, J.A., Nonneman, R.J., Hartmann, J., Moy, S.S., Nicolelis, M.A.*, et al.* (2009). Remote control of neuronal activity in transgenic mice expressing evolved G protein-coupled receptors. Neuron 63, 27-39.

Bennett, G., and Xie, Y. (1988). A peripheral mononeuropathy in rat that produces disorders of pain sensation like those seen in man. Pain 33, 87-107.

Bonetti, E.P., Pieri, L., Cumin, R., Schaffner, R., Pieri, M., Gamzu, E.R., Muller, R.K., and Haefely, W. (1982). Benzodiazepine antagonist Ro 15-1788: neurological and behavioral effects. Psychopharmacology (Berl) 78, 8-18.

Brenner, D.S., Golden, J.P., and Gereau, R.W.t. (2012). A novel behavioral assay for measuring cold sensation in mice. PLoS One 7, e39765.

Copeland, N.G., Jenkins, N.A., and Court, D.L. (2001). Recombineering: a powerful new tool for mouse functional genomics. Nat Rev Genet 2, 769-779.

Dugue, G.P., Brunel, N., Hakim, V., Schwartz, E., Chat, M., Levesque, M., Courtemanche, R., Lena, C., and Dieudonne, S. (2009). Electrical coupling mediates tunable low-frequency oscillations and resonance in the cerebellar Golgi cell network. Neuron 61, 126-139.

Punnakkal, P., von Schoultz, C., Haenraets, K., Wildner, H., and Zeilhofer, H.U. (2014). Morphological, Biophysical and Synaptic Properties of Glutamatergic Neurons of the Mouse Spinal Dorsal Horn. J Physiol 592, 759-776.

Seidler, B., Schmidt, A., Mayr, U., Nakhai, H., Schmid, R.M., Schneider, G., and Saur, D. (2008). A Cre-loxP-based mouse model for conditional somatic gene expression and knockdown in vivo by using avian retroviral vectors. Proc Natl Acad Sci U S A 105, 10137-10142.

Weinberg, M.S., Samulski, R.J., and McCown, T.J. (2013). Adeno-associated virus (AAV) gene therapy for neurological disease. Neuropharmacology 69, 82-88.